# Relationship between Clinical Indicators and the Total Amount of Bacteria in the Tongue Coat Assessed by Real-time PCR in Oral Care Evaluation

Mitsuo KISHI, Masahiro TAKAHASHI, Kayo KISHI*, Fumiko HAREYAMA**, Kohei TAMURA, Akiko ABE, Go SUGIURA, Fumie AIZAWA and Masami YONEMITSU

Department of Preventive Dentistry, Iwate Medical University School of Dentistry
*Department of Oral Microbiology, Iwate Medical University School of Dentistry
**Association of Iwate Dental Hygienist

**Abstract** : We assessed the relationship between clinical and bacteriological indicators on the efficacy of oral care. The subjects comprised 27 patients of a rehabilitation hospital in Iwate prefecture. We evaluated the oral status of the subjects clinically via inspection of the tongue coat volume (tongue coat score), CPI, and measurement of oral malodor (VSC : $H_2S$ and $CH_3SH$ levels). Subsequently, tongue coat samples were collected from the subjects for biological assessment. These samples were weighed and applied to real-time PCR to quantify the total bacterial cells. Examinations were performed both on admission and two months after admission.

At two months after admission, clinical indicators were improved, especially the tongue coat score, CPI, and $CH_3SH$ level. For the bacteriological indicators, the tongue coat volume was reduced significantly and the mean number of bacterial cells in the whole tongue coat sample tended to decrease. However, the mean number of bacterial cells per 1 mg of tongue coat was almost the same. A correlation was observed between the $H_2S$ level and the number of bacterial cells per 1 mg of tongue coat. In step-wise multiple regression models in which the dependent variable was the number of bacterial cells in the whole tongue coat, the tongue coat score and $H_2S$ level were both significant variables. In conclusion, assessment of the tongue coat volume and oral malodor via the $H_2S$ level were efficient clinical indicators to deduce bacteriological changes after oral care.

J Dent Hlth 56 : 665－672, 2006

**Key words** : **Oral care, Tongue coat, Oral malodor, Real-time PCR**

*Reprint requests to* M. KISHI, Department of Preventive Dentistry, Iwate Medical University School of Dentistry, 1-3-27, Chuo-dori, Morioka 020-8505, Japan
TEL : 019-651-5111 (ext. 4516)/FAX : 019-622-2228/E-mail : mkishi@iwate-med.ac.jp

*Oral Microbiology Immunology 2006: 21: 283–288*
*Printed in Singapore. All rights reserved*



ORAL MICROBIOLOGY
AND IMMUNOLOGY

# Resistance to acidic and alkaline environments in the endodontic pathogen *Enterococcus faecalis*

**K. Nakajo, R. Komori, S. Ishikawa, T. Ueno, Y. Suzuki, Y. Iwami, N. Takahashi**
Division of Oral Ecology and Biochemistry, Department of Oral Biology, Tohoku University Graduate School of Dentistry, Sendai, Japan

*Nakajo K, Komori R, Ishikawa S, Ueno T, Suzuki Y, Iwami Y, Takahashi N. Resistance to acidic and alkaline environments in the endodontic pathogen* Enterococcus faecalis. *Oral Microbiol Immunol 2006: 21: 283–288.* © Blackwell Munksgaard, 2006.

**Background/aims:** This study aimed to investigate the biochemical mechanisms employed by the endodontic pathogen *Enterococcus faecalis* to confer acid- and alkali-resistance and to compare these with the mechanisms of representative oral streptococci.
**Methods:** *E. faecalis* JCM8728, *Streptococcus mutans* NCTC10449 and *Streptococcus sanguinis* ATCC10556 were used to assess both acid- and alkali-resistance by examining: (i) growth in complex media; (ii) stability of intracellular pH ($pH_{in}$); (iii) cell durability to leakage of preloaded BCECF (2′,7′-bis-(2-carboxyethyl)-5,6-carboxy-fluorescein); and (iv) cell permeability to SYTOX-Green.
**Results:** Growth was initiated by *E. faecalis* at pH 4.0–11.0, by *S. mutans* at pH 4.0–9.0 and by *S. sanguinis* at pH 5.0–9.0. The $pH_{in}$ was similar to the extracellular pH in *S. mutans* and *S. sanguinis* at pH 5–10, while the $pH_{in}$ of *E. faecalis* was maintained at approximately 7.5–8.5 when extracellular pH was 7.5–10 and was maintained at levels equivalent to the extracellular pH when pH < 7.5. Cell membranes of *E. faecalis* were resistant to BCECF leakage when extracellular pH was 2.5–12 and to SYTOX-Green permeability at pH 4–10. The cell membrane durability to extracellular pH in *E. faecalis* was higher than that observed in the *Streptococcus* strains.
**Conclusion:** Compared to *S. mutans*, *E. faecalis* was found to be equally resistant to acid and more resistant to alkalis. The results suggest that pH-resistance in *E. faecalis* is attributed to membrane durability against acid and alkali, in addition to cell membrane-bound proton-transport systems. These characteristics may account for why *E. faecalis* is frequently isolated from acidic caries lesions and from persistently infected root canals where calcium hydroxide medication is ineffective.

Key words: acid-resistance; alkali-resistance; endodontic pathogen; *Enterococcus faecalis*

Nobuhiro Takahashi, Division of Oral Ecology and Biochemistry, Tohoku University Graduate School of Dentistry, 4-1 Seiryo-machi, Aoba-ku, Sendai 980-8575, Japan
Tel.: +81 22 717 8294;
fax: +81 22 717 8297;
e-mail: nobu-t@mail.tains.tohoku.ac.jp
Accepted for publication February 23, 2006

*Enterococcus faecalis* is a gram-positive facultative anaerobe found among the commensal microflora of the human intestinal tract. Although the prevalence of *E. faecalis* in root canals was already reported in 1959 (47), this bacterium has recently attracted the attention of dental researchers because it has been isolated frequently from dentin caries and from infected root canals (12, 29, 40, 41). Furthermore, several studies have demonstrated that *E. faecalis* is one of the most commonly isolated bacteria in failed endodontic cases treated with calcium hydroxide [$Ca(OH)_2$] (12, 43). Indeed, this bacterium appears to be highly resistant to $Ca(OH)_2$ (5, 6), which is known as one of the most effective endodontic medicaments because of the bactericidal effect derived from its strong alkaline properties (42). These findings suggest that *E. faecalis* is resistant to both acid environments, such as those of carious dentin including root canals, and alkaline environments such as those of root canals treated with $Ca(OH)_2$.

Several mechanisms have been proposed regarding the methods employed by *E. faecalis* to survive extremes in the pH environment. It has been known that *E. faecalis* can grow at pH 9.6 since the 1930s (39). In recent years, *E. faecalis* has been demonstrated to synthesize a variety of stress proteins when exposed to acids (8) and alkalis (7). However, stress protein synthesis by *E. faecalis* appears to be unrelated to survival at extreme pHs, such as the alkali pH induced by $Ca(OH)_2$ treatment (6, 7). Instead, it is suggested

that a cell membrane-bound proton-transport system is critical to survival under these conditions (6).

Kakinuma and Igarashi (17–20) proposed that an ATP-linked potassium/proton antiport system incorporates protons into the cells to maintain the intracellular pH ($pH_{in}$) in alkaline environments, as has been observed in *Enterococcus hirae*, an enterococcal species similar to *E. faecalis*. On the other hand, acid-resistance in *E. faecalis* is the result of the activity of the cell membrane-bound proton-translocating ATPase ($H^+$-ATPase) which maintains $pH_{in}$ by excreting protons from the cells (22). These findings show that cell membrane-bound proton-transport systems are responsible for acid- and alkali-resistance, but for them to function, the bacterium has to produce energy, such as ATP, continuously. However, in treated root canal environments where the pH is maintained at approximately 9.5–11.0 with $Ca(OH)_2$ (2, 33) and nutrients appear to be limited, it should be difficult for the bacterium to obtain sufficient energy through metabolism. To overcome this situation, the bacterium may have additional mechanisms to protect itself from pH impairment.

This study was undertaken to elucidate the biochemical mechanisms associated with acid- and alkali-resistance, excluding those that use ATP-linked proton-transport systems, in non-growing and non-metabolizing *E. faecalis* cells by comparing them with those of representative oral streptococci, *Streptococcus mutans* and *Streptococcus sanguinis*.

## Material and methods

### Bacterial strains and culture media

*E. faecalis* JCM8728, *S. mutans* NCTC10449 and *S. sanguinis* ATCC10556 were used in this study. These bacteria were cultured on a complex medium (10) containing 1.7% tryptone (Difco Laboratories, Detroit, MI), 0.3% yeast extract (Difco Laboratories) and 0.5% NaCl, which was autoclaved before 0.5% glucose and 50 mM potassium phosphate buffer were added using a sterile membrane filter (pore size 0.22 μm; Pall Corporation, East Hills, NY) (TYG culture medium). This medium was also used as a pre-culture medium.

### Growth ability at acidic and alkali pH

Each strain was inoculated in TYG culture medium and pre-cultured at 37°C overnight. The cell culture was transferred (5% inoculum size) to TYG culture media adjusted to pH 3.0–11.0 with HCl or KOH and incubated at 37°C for 48 h. Bacterial growth was conducted in an anaerobic glove box (90% $N_2$ and 10% $H_2$, NH-type; Hirasawa Works, Tokyo, Japan) and was estimated at 48 h after inoculation by measuring optical density at 660 nm ($OD_{660}$) with a spectrophotometer (UV-160, Shimadzu Corporation, Kyoto, Japan). Initial and final pH values of the cell cultures were determined using a pH meter (Model HM-30G, DKK-TOA Corporation, Tokyo, Japan). Bacterial purity was confirmed after each experiment by culturing on blood agar plates.

### The $pH_{in}$ at acidic and alkali pH

The $pH_{in}$ at acidic and alkali pH was estimated using the methods of Futsaether et al. (9) and Iwami et al. (16). Each strain was grown in TYG culture medium at pH 7.0 until the late-log growth phase ($OD_{660}$ 0.9–1.0) in another anaerobic glove box (80% $N_2$, 10% $H_2$ and 10% $CO_2$, NHC-type; Hirasawa Works). The culture was then taken from the glove box, mixed with 2′,7′-bis-(2-carboxyethyl)-5,6-carboxy-fluorescein acetoxymethyl ester (BCECF-AM, Dojindo Laboratories, Kumamoto, Japan) at a final concentration of 0.5 μM and incubated for 15 min at 35°C (16). The BCECF-loaded cells were harvested and washed three times by centrifugation (21,000 ***g*** for 7 min at 4°C) with deionized water. BCECF-AM easily penetrates the cell membrane because of its hydrophobicity, but BCECF, the hydrolyzed product arising from intracellular esterases, is retained within the cells and exhibits fluorescence (9, 32). The cells were suspended in deionized water at an $OD_{660}$ of 5.0 (16).

The BCECF-loaded cell suspensions were diluted in the presence of 150 mM KCl and 0.5 mM 3-(*N*-morpholino)propanesulfonic acid (MOPS)–KOH buffer (pH 7.0) for experiments at acidic pH, or 0.5 mM *N*,*N*-bis(2-hydroxyethyl)glycine (Bicine)–KOH buffer (pH 7.5) for experiments at alkali pH. The cell suspensions were then incubated for 30 min at 37°C for the depletion of intracellular polysaccharide. The cells were pelleted by centrifugation (21,000 ***g*** for 5 min at room temperature) and stored at 4°C until use.

The reaction mixtures containing BCECF-loaded cells ($OD_{660}$ 1.0), 150 mM KCl and 0.5 mM MOPS–KOH buffer (pH 7.0) or 0.5 mM Bicine–KOH buffer (pH 7.5), were incubated at 37°C with agitation by a magnetic stirrer. Small aliquots of 0.15 M HCl or 0.15–0.8 M KOH were added to the reaction mixture to decrease or increase extracellular pH between 4.0 and 10.0 at intervals of 4 min. The pH of the reaction mixture, and the fluorescence intensity derived from intracellular BCECF were monitored simultaneously using a pH meter and a fluorescence spectrophotometer (Model CAF-110, JASCO Corporation, Tokyo, Japan) at excitation and emission wavelengths of 500 and 540 nm, respectively.

The values of $pH_{in}$ were calculated using the calibration curve for fluorescence intensity. To obtain fluorescence intensities at various $pH_{in}$, HCl or KOH were added to the reaction mixture containing the cells ($OD_{660}$ 1.0), 150 mM KCl, 0.5 mM MOPS–KOH buffer (pH 7.0) or 0.5 mM Bicine–KOH buffer (pH 7.5) and 12 μM nigericin which eliminates the pH gradient across the bacterial cell membrane (4, 9, 13, 25, 46). Using this method, $pH_{in}$ became the same as the extracellular pH and could then be measured using a pH meter. Separate calibration curves were prepared for individual experiments (15).

### BCECF leakage at acidic and alkali pH

The BCECF-loaded cells were prepared as described for the investigation of $pH_{in}$ at acidic and alkali pH. BCECF is retained within the cells when their cell membranes remain intact, but the fluorescent dye leaks out easily when the cell membranes are damaged. Consequently, leakage of BCECF from cells could be used as one of the determinants of cell membrane durability.

The cells were resuspended in 150 mM KCl and 0.5 mM MOPS–KOH buffer (pH 7.0) or 0.5 mM Bicine–KOH buffer (pH 7.5) at an $OD_{660}$ of 1.0, and incubated at 35°C with agitation by a magnetic stirrer. Within 2 min of starting incubation, the reaction mixture was adjusted to pH 2.0–12.0 with small aliquots of 0.15 M HCl or 0.15–0.8 M KOH. After an additional incubation of 8 min, the reaction mixture was centrifuged (21,000 ***g*** for 5 min at room temperature). Cell pellets were suspended in 100 mM 3-(cyclohexylamino)-2-hydroxy-1-propanesulfonic acid (CHES)–KOH buffer (pH 10.0), 1.25 M KCl and 10 μM nigericin and stored at room temperature overnight. The fluorescence intensity of residual BCECF in the cells was determined fluorometrically.

### SYTOX-Green permeability at acidic and alkali pH

Each bacterial strain was grown, harvested, washed and starved as described in the

investigation of $pH_{in}$ at acidic and alkaline pHs, except for the BCECF loading. The cells were resuspended in 150 mM KCl and 0.5 mM MOPS–KOH buffer (pH 7.0) or 0.5 mM Bicine–KOH buffer (pH 7.0) at $OD_{660}$ of 1.0, and incubated at 35°C with agitation by a magnetic stirrer. Within 2 min of starting incubation, the reaction mixture was adjusted to pH 4.0–10.0 with small aliquots of 0.15 M HCl or 0.15–0.8 M KOH. After adding SYTOX-Green (Molecular Probe Inc., Eugene, OR) at a final concentration of 2.5 μM, the reaction mixture was further incubated for 5 min; SYTOX-Green permeates damaged cell membranes and binds to nucleic acids where it fluoresces. Consequently, the penetration of SYTOX-Green can be used to evaluate cell membrane durability. The fluorescence intensity of SYTOX-Green bound to nucleic acids was determined fluorometrically at excitation and emission wavelengths of 504 and 540 nm, respectively.

## Results

### Growth ability at acidic and alkali pH

*E. faecalis*, *S. mutans* and *S. sanguinis* were able to grow at an initial pH of 4.0–11.0 (Fig. 1A-1), pH 4.0–9.0 (Fig. 1B-1) and pH 5.0–9.0 (Fig. 1C-1), respectively. The *E. faecalis* grew well over a wide pH range, whereas *S. mutans* and *S. sanguinis* grew well in the narrow pH range around neutral. The culture pH decreased by 0.0–2.9 pH units during 48 h of growth (Fig. 1A-2, B-2 and C-2). At an initial pH of 11, for example, *E. faecalis* decreased the culture pH to 10.5, while at an initial pH of 9.0, *S. mutans* and *S. sanguinis* decreased the culture pH to 8.1 and 7.8, respectively.

### The $pH_{in}$ at acidic and alkali pH

When extracellular pH was between 8 and 10, $pH_{in}$ was equal to the extracellular pH in *S. sanguinis*, slightly lower than the extracellular pH in *S. mutans* and stable at approximately 7.5–8.5 in *E. faecalis* (Fig. 2). When extracellular pH was between 5 and 7.5, $pH_{in}$ was similar to the extracellular pH in all the strains. When extracellular pH was between 4 and 5, $pH_{in}$ was maintained at approximately 5 in *S. mutans*, and was equal to the extracellular pH in *S. sanguinis*. However, $pH_{in}$ of *E. faecalis* at an extracellular pH < 5 could not be estimated because the background fluorescence of *E. faecalis* masked the signal fluorescence of $pH_{in}$.

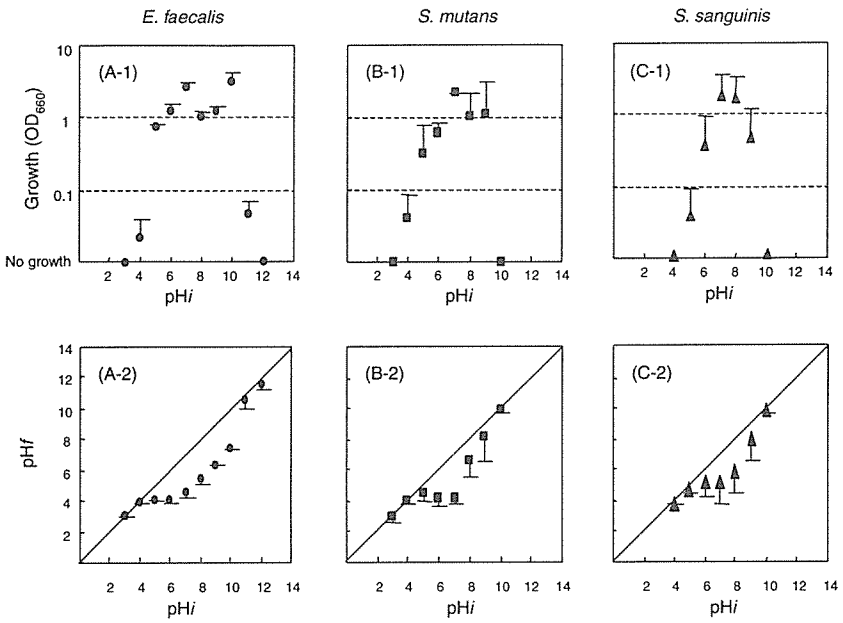


*Fig. 1.* Bacterial growth of *Enterococcus faecalis* JCM 8728 (A-1), *Streptococcus mutans* NCTC 10449 (B-1) and *Streptococcus sanguinis* ATCC 10556 (C-1) at various initial pH levels (pH*i*) in TYG culture media, and final pHs (pH*f*) after 48 h of growth of *E. faecalis* JCM 8728 (A-2), *S. mutans* NCTC 10449 (B-2) and *S. sanguinis* ATCC 10556 (C-2). Data were given in the means with standard deviation obtained from three independent experiments. Bacterial culture with $OD_{660}$ < 0.03 was judged as no growth.

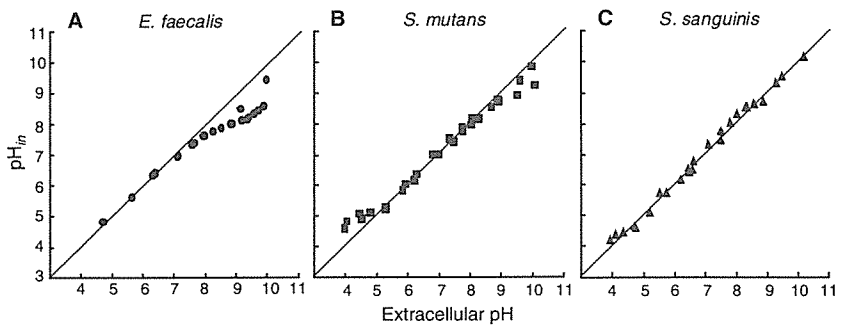


*Fig. 2.* The $pH_{in}$ of *Enterococcus faecalis* JCM 8728 (A), *Streptococcus mutans* NCTC 10449 (B) and *Streptococcus sanguinis* ATCC 10556 (C) at various extracellular pH values. All the data obtained from three independent experiments were plotted.

### BCECF leakage at acidic and alkali pHs

*E. faecalis* was resistant to BCECF leakage when extracellular pH was 2.5–12 (Fig. 3A) with residual BCECF > 80%. Both *S. mutans* and *S. sanguinis* were resistant within the pH range of 4–10 (Fig. 3B,C), although *S. mutans* appeared to be more resistant than *S. sanguinis* at alkali pH.

### SYTOX-Green permeability at acidic and alkali pH

The *E. faecalis* was resistant to permeation by SYTOX-Green at an extracellular pH between 4 and 10 and showed low and constant fluorescence intensities (Fig. 4A). Both *S. mutans* and *S. sanguinis* were resistant at pH 5–9 (Fig. 4B,C), although their fluorescence intensities were higher than those of *E. faecalis*. At pH > 9 and <5, both *S. mutans* and *S. sanguinis* showed high permeability to SYTOX-Green (Fig. 4B,C).

## Discussion

In this study, *E. faecalis* was observed to be more alkali-resistant in growth than either *S. mutans* or *S. sanguinis*, and in terms of the acid-resistance of its growth this bacterium showed similar acid-resistance to *S. mutans* and more acid-resist-

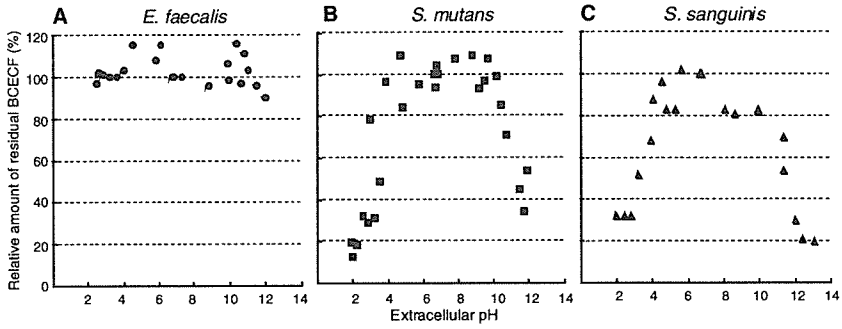


*Fig. 3.* The percentage of residual intracellular BCECF in *Enterococcus faecalis* JCM 8728 (A), *Streptococcus mutans* NCTC 10449 (B) and *Streptococcus sanguinis* ATCC 10556 (C) at various extracellular pH levels. The value at pH 7.0 was regarded as 100. All data obtained from three independent experiments were plotted.

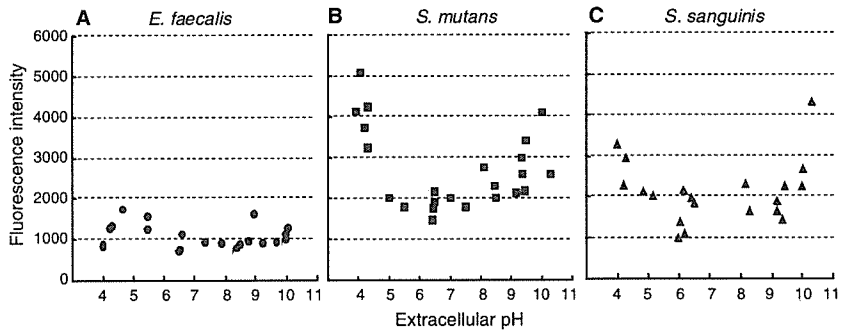


*Fig. 4.* Fluorescence intensity of SYTOX-Green into the cells for 5 min of *Enterococcus faecalis* JCM 8728 (A), *Streptococcus mutans* NCTC 10449 (B) and *Streptococcus sanguinis* ATCC 10556 (C) at various extracellular pH levels. All the data obtained from three independent experiments were plotted.

ance than *S. sanguinis* (Fig. 1). Although the culture pH decreased during growth, initial culture pH is thought to be critical for these bacteria to initiate growth. It was reported that *E. faecalis*, *S. mutans* and *S. sanguinis* initiated growth at pH 5.0, 5.0 and 5.5, respectively (14). The most alkali pH for *E. faecalis* to initiate growth was reported to be approximately 10 (28, 29, 39), but these values for *S. mutans* and *S. sanguinis* were determined for the first time in the present study. In general, the results of the present study were consistent with those previous reports, but the bacterial species in the present study appeared to be more pH-resistant than those in the previous studies. This discrepancy could be the result of differences among bacterial strains and among growth conditions, including the culture media.

The bacterial growth yields were different among the initial pH values (Fig. 1). The growth yield may be influenced by a change in metabolic pathway, an accumulation of end products and a limitation of energy source although these possibilities need to be elucidated. Growth medium composition such as the concentration and type of buffer may also influence bacterial growth and change in culture pH during growth.

Bacteria need to maintain their $pH_{in}$ against extracellular pH extremes for survival. Many mechanisms by which $pH_{in}$ is maintained relative to extracellular alkaline pH values have been reported. Kakinuma and Igarashi (17–20) proposed that in *E. faecalis* an ATP-linked potassium/proton antiport system functions to incorporate protons into cells against intracellular alkalization. In addition, Evans et al. (6) have demonstrated that a protonophore, carbonyl cyanide *m*-chlorophenylhydrazone (CCCP), diminished alkali-resistance of *E. faecalis*, supporting the involvement of a cell membrane-bound proton-transport system in the alkali-resistance. Since the potassium/proton antiport system requires ATP to function, *E. faecalis* needs to generate ATP by metabolizing energy sources at alkali pH. Not only can *E. faecalis* ferment carbohydrates but it can also degrade proteins such as gelatin (21). Thus, it could be possible that *E. faecalis* obtains energy from nitrogenous compounds available in the root canals and so drives an ATP-linked proton-transport system. However, under conditions such as those found in root canals after endodontic therapy using $Ca(OH)_2$, it is unlikely that metabolic substrate is supplied sufficiently. Consequently, the potassium/proton antiport system is unlikely to function efficiently and additional mechanisms are thought to be involved.

In the present study, *E. faecalis* was able to maintain its $pH_{in}$ at approximately 8–8.5 when extracellular pH was 7.5–10 in the absence of energy sources, namely without an ATP supply (Fig. 2A). In addition, this bacterium exhibited low leakage of cell-loaded BCECF (Fig. 3A) and low permeation of SYTOX-Green (Fig. 4A), indicating that the cell membrane was durable at alkali pH and capable of retaining small intracellular molecules without leakage. This ability to maintain $pH_{in}$ and protect cell membranes from alkali-impairment may enable *E. faecalis* to survive extreme alkaline environments, such as those of a root canal medicated with $Ca(OH)_2$, without energy substrates. Perez et al. (33) demonstrated that dentinal pH decreased to around 9.5 within 2–3 weeks after placement of $Ca(OH)_2$ in root canals. At this pH, *E. faecalis* would not only survive but it would grow again when metabolic substrates were supplied (Fig. 1A).

In *S. mutans* and *S. sanguinis*, however, $pH_{in}$ was not maintained (Fig. 2B,C), and cell-loaded BCECF leaked out from cells (Fig. 3B,C) and SYTOX-Green permeated into cells (Fig. 4B,C) at alkali pH. These observations indicate that the cell membranes of these streptococci are more vulnerable to alkaline environments than the membrane of *E. faecalis*, resulting in the alkali-labile growth in *S. mutans* and *S. sanguinis* (Fig. 1B,C).

The cell membrane of *E. faecalis* was highly acid-durable (Figs 3A and 4A), suggesting that the capacity for acid-resistant growth (Fig. 1A) is attributed to the acid-durability of the cell membrane, although the $pH_{in}$ maintenance at an extracellular pH < 5 could not be determined. While *S. mutans* had lower acid-durability of cell membrane than *E. faecalis* (Figs 3B and 4B), this bacterium maintained its $pH_{in}$ at approximately 5 when extracellular pH was <5 without an energy source (Fig. 2B). This $pH_{in}$ stability may compensate for the acid-durability of the cell membrane, which is weakened at an extracellular pH < 5 (Figs 3B and 4B), and contributes to acid-resistant growth in *S. mutans* (Fig. 1B). In the present study, however, the mechanism of the $pH_{in}$ stability was not elucidated.

In addition, *E. faecalis*, *S. mutans* and *S. sanguinis* are known to have $H^+$-ATPase which functions to maintain $pH_{in}$ at acidic extracellular pH by expelling protons from cells when ATP is supplied; the pH minima for $H^+$-ATPase activity in these bacteria are 4.0, 4.0 and 4.5, respectively (3). The most acidic pH values for these bacteria to initiate growth (Fig. 1) appeared to reflect these pH minima, suggesting that $H^+$-ATPase can confer acid resistance on these bacteria in the presence of energy sources (22).

Although both *E. faecalis* and *S. mutans* were found to be acid-resistant in this study, they are isolated from different oral acidic sites; *S. mutans* has frequently been isolated from dental plaque and dental caries, including enamel caries, dentin caries and infected root canals (24, 30, 38), while *E. faecalis* has not usually been isolated from dental plaque (11) or enamel caries (31), but is mainly isolated from dentin caries including infected root canals (27, 29, 35, 41, 43). The discrepancy in the distribution of these two bacterial species could be the result of the different extent to which they adhere to tooth surfaces; *S. mutans* is known to colonize the enamel of the tooth surface and promote plaque formation (1, 26, 34, 45), whereas the ability of *E. faecalis* is still unclear. While both bacteria are capable of adhering to type I collagen consisting of dentin (36, 37, 44), *E. faecalis* is more adhesive to dentin and invasive of dentinal tubules than *S. mutans* (23, 36), possibly accounting for the relatively increased frequency of isolation of *E. faecalis* from dentin caries and infected root canals.

In conclusion, the present study demonstrated that *E. faecalis* was similar in acid-resistance to *S. mutans*, but more alkali-resistant than *S. mutans* and *S. sanguinis*. The high acid- and alkali-resistance observed in *E. faecalis* could be the result of cell membrane durability against acid and alkaline substances, in addition to ATP-linked proton-transport system functioning. The pH-resistance of *E. faecalis* may account for why this bacterium is frequently isolated from both acidic caries lesions and persistently infected root canals treated with $Ca(OH)_2$ medicaments.

## Acknowledgments

This study was supported in part by Grants-in-Aid for Scientific Research (no. 16390601, no. 17659659, no. 17791350) from the Ministry of Education, Culture, Sports, Science and Technology, Japan.

## References

1. Aoki H, Shiroza T, Hayakawa M, Sato S, Kuramitsu HK. Cloning of a *Streptococcus mutans* glucosyltransferase gene coding for insoluble glucan synthesis. Infect Immun 1986: **53**: 587–594.
2. Ardeshna S, Qualtrough A, Worthington H. An *in vitro* comparison of pH changes in root dentine following canal dressing with calcium hydroxide points and a conventional calcium hydroxide paste. Int Endod J 2002: **35**: 239–244.
3. Bender GR, Sutton SVW, Marquis RE. Acid tolerance, proton permeability, and membrane ATPases of oral streptococci. Infect Immun 1986: **53**: 331–338.
4. Distler W, Kagermeier A, Hickel R, Krönke A. Lactate influx and efflux in the '*Streptococcus mutans* group' and *Streptococcus sanguis*. Caries Res 1989: **23**: 252–255.
5. Engström B. The significance of enterococci in root canal treatment. Odontologisk Revy 1964: **15**: 87–106.
6. Evans M, Davies JK, Sundqvist G, Figdor D. Mechanisms involved in the resistance of *Enterococcus faecalis* to calcium hydroxide. Int Endod J 2002: **35**: 221–228.
7. Flahaut S, Hartke A, Giard JC, Auffray Y. Alkaline stress response in *Enterococcus faecalis*: adaptation, cross-protection, and changes in protein synthesis. Appl Environ Microbiol 1997: **63**: 812–814.
8. Flahaut S, Hartke A, Giard JC, Benachour A, Boutibonnes P, Auffray Y. Relationship between stress response towards bile salts, acid and heat treatment in *Enterococcus faecalis*. FEMS Microbiol Lett 1996: **138**: 49–54.
9. Futsaether CM, Kjeldstad B, Johnsson A. Measurement of the intracellular pH of *Propionibacterium acnes*: comparison between the fluorescent probe BCECF and 31P-NMR spectroscopy. Can J Microbiol 1993: **39**: 180–186.
10. Gauthier L, Vadeboncoeur C, Mayrand D. Loss of sensitivity to xylitol by *Streptococcus mutans* LG-1. Caries Res 1984: **18**: 289–295.
11. Guggenheim B. Streptococci of dental plaques. Caries Res 1968: **2**: 147–163.
12. Hancock H, Sigurdsson A, Trope M, Moiseiwitsch J. Bacteria isolated after unsuccessful endodontic treatment in a North American population. Oral Surg Oral Med Oral Pathol Oral Radiol Endod 2001: **91**: 579–586.
13. Harold FM, Pavlasova E, Baarda JR. A transmembrane pH gradient in *Streptococcus faecalis*. Origin and dissipation by proton conductors and *N,N*-dicyclo-hexylcarbodiimide. Biochem Biophys Acta 1970: **196**: 235–244.
14. Harper DS, Loesche WJ. Growth and acid tolerance of human dental plaque bacteria. Arch Oral Biol 1984: **29**: 843–848.
15. Hegyi P, Rakonczay Z, Gray MA, Argent BE. Measurement of intracellular pH in pancreatic duct cells: a new method for calibrating the fluorescence data. Pancreas 2004: **28**: 427–434.
16. Iwami Y, Kawarada K, Kojima I et al. Intracellular and extracellular pHs of *Streptococcus mutans* after addition of acids: loading and efflux of a fluorescent pH indicator in streptococcal cells. Oral Microbiol Immunol 2002: **17**: 239–244.
17. Kakinuma Y. Lowering of cytoplasmic pH is essential for growth of *Streptococcus faecalis* at high pH. J Bacteriol 1987: **169**: 4403–4405.
18. Kakinuma Y, Igarashi K. Mutants of *Streptococcus faecalis* sensitive to alkaline pH lack $Na^+$-ATPase. J Bacteriol 1990: **172**: 1732–1735.
19. Kakinuma Y, Igarashi K. Potassium/proton antiport system of growing *Enterococcus hirae* at high pH. J Bacteriol 1995: **177**: 2227–2229.
20. Kakinuma Y, Igarashi K. Isolation and properties of *Enterococcus hirae* mutants defective in the potassium/proton antiport system. J Bacteriol 1999: **181**: 4103–4105.
21. Kayaoglu G, Orstavik D. Virulence factors of *Enterococcus faecalis*: relationship to endodontic disease. Crit Rev Oral Biol Med 2004: **15**: 308–320.
22. Kobayashi H. A proton-translocating ATPase regulates pH of the bacterial cytoplasm. J Biol Chem 1985: **260**: 72–76.
23. Love RM. *Enterococcus faecalis* – a mechanism for its role in endodontic failure. Int Endod J 2001: **34**: 399–405.
24. Love RM, Jenkinson HF. Invasion of dentinal tubules by oral bacteria. Crit Rev Oral Biol Med 2002: **13**: 171–183.
25. Loveren CV, Fielmich AM, Brink BT. Comparison of the effects of fluoride and the ionophore nigericine on acid production by *Streptococcus mutans* and the resultant *in vitro* enamel demineralization. J Dent Res 1987: **66**: 1658–1662.
26. Matsumura M, Izumi T, Matsumoto M, Tsuji M, Fujiwara T, Ooshima T. The role of glucan-binding proteins in the cariogenicity of *Streptococcus mutans*. Microbiol Immunol 2003: **47**: 213–215.
27. Molander A, Reit C, Dahlén G, Kvist T. Microbiological status of root-filled teeth with apical periodontitis. Int Endod J 1998: **31**: 1–7.
28. Mundt JO. Enterococci. In: Sneath PHA, Mair NS, Sharpe ME, Holt JG, eds. Bergey's manual of systematic bacteriology, Vol. 2. Baltimore, MD: Williams & Wilkins, 1986: 1063–1065.
29. Nakajo K, Nakazawa F, Iwaku M, Hoshino E. Alkali-resistant bacteria in root canal systems. Oral Microbiol Immunol 2004: **19**: 390–394.
30. Nascimento MM, Hofling JF, Goncalves RB. *Streptococcus mutans* genotypes isolated from root and coronal caries. Caries Res 2004: **38**: 454–463.
31. Nyvad B, Kilian M. Comparison of the initial streptococcal microflora on dental enamel in caries-active and in caries-inactive individuals. Caries Res 1990: **24**: 267–272.
32. Paradiso AM, Tsien RY, Machen TE. $Na^+$-$H^+$ exchange in gastric glands as measured with a cytoplasmic-trapped, fluorescent pH indicator. Proc Natl Acad Sci U S A 1984: **81**: 7436–7440.

33. Perez F, Franchi M, Peli J. Effect of calcium hydroxide form and placement on root dentine pH. Int Endod J 2001: **34**: 417–423.
34. Pieringer RA. The metabolism of glyceride glycolipids. I. Biosynthesis of monoglucosyl diglyceride and diglucosyl diglyceride by glucosyltransferase pathways in *Streptococcus faecalis*. J Biol Chem 1968: **243**: 4894–4903.
35. Pinheiro ET, Gomes BP, Ferraz CC, Sousa EL, Teixeira FB, Souza-Filho FJ. Microorganisms from canals of root-filled teeth with periapical lesions. Int Endod J 2003: **36**: 1–11.
36. Rich RL, Kreikemeyer B, Owens RT et al. Ace is a collagen-binding MSCRAMM from *Enterococcus faecalis*. J Biol Chem 1999: **274**: 26939–26945.
37. Sato Y, Okamoto K, Kagami A, Yamamoto Y, Igarashi T, Kizaki H. *Streptococcus mutans* strains harboring collagen-binding adhesin. J Dent Res 2004: **83**: 534–539.
38. Sansone C, Van Houte J, Joshipura K, Kent R, Margolis HC. The association of mutans streptococci and non-mutans streptococci capable of acidogenesis at a low pH with dental caries on enamel and root surfaces. J Dent Res 1993: **72**: 508–516.
39. Sherman JM. The streptococci. Bacteriol Rev 1937: **1**: 3–97.
40. Siqueira JF, Uzeda M. Disinfection by calcium hydroxide paste of dentinal tubules infected with two obligate and one facultative anaerobic bacteria. J Endod 1996: **22**: 674–676.
41. Siren E, Haapasalo M, Ranta K, Salmi P, Kerosuo E. Microbiological findings and clinical treatment procedures in endodontic cases selected for microbiological investigation. Int Endod J 1997: **30**: 91–95.
42. Sjögren U, Figdor D, Spångberg L, Sundqvist G, The antimicrobial effect of calcium hydroxide as a short-term intracanal dressing. Int Endod J 1991: **24**: 119–125.
43. Sundqvist G, Figdor D, Persson S, Sjögren U. Microbiologic analysis of teeth with failed endodontic treatment and the outcome of conservative re-treatment. Oral Surg Oral Med Oral Pathol Oral Radiol Endod 1998: **85**: 86–93.
44. Switalski LM, Patti JM, Butcher W, Gristina AG, Speziale P, Hook M. A collagen receptor on *Staphylococcus aureus* strains isolated from patients with septic arthritis mediates adhesion to cartilage. Mol Microbiol 1993: **7**: 99–107.
45. Tamesada M, Kawabata S, Fujiwara T, Hamada S. Synergistic effects of streptococcal glucosyltransferases on adhesive biofilm formation. J Dent Res 2004: **83**: 874–879.
46. Tsujimoto K, Semadani M, Huflejt M, Packer L. Intracellular pH of halobacteria can be determined by the fluorescent dye 2′,7′-bis (carboxyethyl)-5(6)-carboxyfluorecein. Biochem Biophys Res Commun 1988: **155**: 123–129.
47. Winkler KC, Amerongen JV. Bacteriologic results from 4,000 root canal cultures. Oral Surg Oral Med Oral Pathol 1959: **12**: 857–875.

*Oral Microbiology Immunology 2006: 21: 201–205*
*Printed in Singapore. All rights reserved*



ORAL MICROBIOLOGY AND IMMUNOLOGY

# Difference in the xylitol sensitivity of acid production among *Streptococcus mutans* strains and the biochemical mechanism

**H. Miyasawa-Hori[1], S. Aizawa[2], N. Takahashi[1]**
[1]Division of Oral Ecology and Biochemistry, Department of Oral Biology and [2]Division of Pediatric Dentistry, Department of Lifelong Oral Health Sciences, Tohoku University Graduate School of Dentistry, Sendai, Japan

*Miyasawa-Hori H, Aizawa S, Takahashi N. Difference in the xylitol sensitivity of acid production among* Streptococcus mutans *strains and the biochemical mechanism. Oral Microbiol Immunol 2006: 21: 201–205.* © Blackwell Munksgaard, 2006.

Xylitol inhibits the glycolysis and growth of *Streptococcus mutans*, but to different degrees among strains. Thus, we studied the biochemical mechanism through which the inhibition varies, using *S. mutans* strains ATCC 31989, NCTN 10449, and NCIB 11723, which are highly sensitive, moderately sensitive, and resistant to xylitol, respectively, under strictly anaerobic conditions such as those found in deep layers of dental plaque. Xylitol (30 mM) decreased the rate of acid production from glucose (10 mM) in ATCC 31989, NCTC 10449, and NCIB 11723 by 86, 26, and 0%, respectively. The activities of the xylitol : phosphoenolpyruvate phosphotransferase system (PEP-PTS) relative to those of glucose : PEP-PTS were 120, 16, and 3%, respectively. In ATCC 31989 and NCTC 10449, intracellular accumulation of xylitol 5-phosphate and decreases of fructose 1,6-bisphosphate and glucose 6-phosphate were observed. Furthermore, in the presence of xylitol (30 mM), glucose : PEP-PTS activities decreased by 34, 17, and 0%, respectively. These findings indicated that the higher the xylitol : PEP-PTS activity was and the more effectively xylitol decreased glucose : PEP-PTS activity, the more sensitive the strain was to xylitol. These results suggest that the following inhibitory mechanisms are active in the xylitol-sensitive mutans streptococci: direct inhibition of glycolytic enzymes by xylitol 5-phosphate derived from xylitol : PEP-PTS and, possibly, indirect inhibition through competition for the phosphoryl donor, HPr-P, between glucose and xylitol : PEP-PTSs.

Key words: acid production; phosphoenolpyruvate-sugar phosphotransferase system; *Streptococcus mutans*; xylitol

Nobuhiro Takahashi, Division of Oral Ecology and Biochemistry, Department of Oral Biology, Tohoku University Graduate School of Dentistry, 4–1 Seiryo-machi, Aoba-ku, Sendai, 980–8575, Japan
Tel.: +81 22 7178294;
fax: +81 22 7178297;
e-mail: nobu-t@mail.tains.tohoku.ac.jp
Accepted for publication October 26, 2005

Xylitol is widely used as a noncariogenic sugar substitute because it is not fermented by oral bacteria (6). Xylitol has been reported to inhibit the growth of mutans streptococci in the presence of glucose, galactose, mannose, lactose, maltose, sucrose, sorbitol or mannitol as a carbon source *in vitro* (1, 5, 7, 8, 16, 24, 25), and the acid production from glucose by resting cells of *Streptococcus mutans* (7, 13, 25). Xylitol is also known to selectively inhibit the growth of *S. mutans* in mixed culture using a chemostat (3, 15).

The major route of sugar transport by microorganisms is via the phosphoenolpyruvate phosphotransferase system (PEP-PTS). Two sugar-nonspecific proteins, enzyme-I and histidine-containing phosphocarrier protein (HPr), and a sugar-specific protein, enzyme-II are required for PEP-PTSs. PEP phosphorylates enzyme-I to phospho-enzyme-I, which in turn transfers the phosphoryl group to HPr. In many cases, phospho-HPr (HPr-P) generated from phospho-enzyme-I, transfers the phosphoryl group directly to enzyme-II, which in turn phosphorylates incoming sugar (10, 14).

Bacterial cells are thought to incorporate xylitol as xylitol 5-phosphate through xylitol : PEP-PTS and the xylitol 5-phosphate inhibits the enzyme activity of sugar metabolism, resulting in the inhibition of both bacterial growth and acid production (18). In addition, the futile cycle, in which xylitol 5-phosphate is dephosphorylated to xylitol with waste of PEP potential, can also retard the growth of *S. mutans* (18).

However, some strains are xylitol sensitive whereas others are resistant (19), and the degree of inhibition varies among strains (25). Thus, we studied the biochemical mechanism of the variable inhibition, using three strains of *S. mutans* previously characterized as highly sensitive, moderately sensitive, and resistant to xylitol under strictly anaerobic conditions such as those found in deep layers of dental plaque.

## Material and methods

### Bacterial strains and growth conditions

We used the following strains of *S. mutans*: NCTC 10449, ATCC 31989, and NCIB 11723. *S. mutans* NCTC 10449 was a gift as a xylitol-sensitive strain from Prof. L. Trahan (Université Laval, Québec, Canada) (20). Each strain was inoculated into a complex medium containing 1.7% tryptone (Difco Laboratories, Detroit, MI), 0.3% yeast extract (Difco), 85 mM NaCl, and 11 mM glucose as described (25) under strictly anaerobic conditions in an anaerobic chamber ($N_2$, 80%; $H_2$, 10%; $CO_2$, 10%, NHC-type, Hirasawa Works, Tokyo, Japan) and incubated at 35°C overnight. Cell cultures were transferred into the same complex medium and precultured overnight at 35°C. The cell cultures were again transferred into the same complex medium (5% inoculum size) and grown at 35°C. The bacterial cells were harvested by centrifugation (7000 × *g* for 15 min at 4°C) at an early logarithmic phase of growth (optical density at 660 nm [$OD_{660}$] ≈ 0.3) under anaerobic conditions as described previously (17). Bacterial purity was regularly confirmed by culturing on blood agar plates.

### Acid production from glucose in the presence of xylitol

The following experiments were conducted in a different type of anaerobic chamber ($N_2$, 90%; $H_2$, 10%, NH-type, Hirasawa Works). Cells were washed twice with cold 2 mM potassium phosphate buffer (pH 7.0) containing 150 mM KCl and 5 mM $MgCl_2$, and suspended in the same buffer. The optical density of the cell suspension at 660 nm was adjusted to 3.5 (1.9 mg of cells [dry weight] per ml).

The cell suspensions were agitated with a magnetic stirrer at 35°C. The reaction was started by adding a mixture of 10 mM glucose and 0 or 30 mM xylitol to the cell suspensions. The rate of acid production by the cells was monitored at pH 7.0 using an automatic pH titrator (model AUT-211S, Toa Electronics Ltd, Kobe, Japan) with 50 mM KOH. The rate of acid production at 2 min after adding glucose or the glucose-xylitol mixture was calculated as μmol of protons per min per mg dry weight of cells.

Before and after the incubation for 10 min, cell suspensions (0.9 ml) were sampled and mixed immediately with 0.1 ml of 6 N perchloric acid. The mixtures were filtered (pore size 0.20 μm, polypropylene; ADVANTEC, Toyo Roshi Ltd, Tokyo, Japan) and cell-free filtrates were diluted with 0.2 N hydrochloric acid and stored at 4°C for the assay of acidic end products.

### Analysis of acidic end products

Amounts of acidic end products, lactic, acetic, formic and pyruvic acids were quantified using a carboxylic acid analyzer (model EYELA S-3000X; Tokyo Rikakikai Co., Ltd, Tokyo, Japan) in stored cell-free filtrates, as described previously (17).

### PEP-PTS activities for glucose, xylitol and fructose (glucose, xylitol and fructose : PEP-PTS activities)

The PEP-PTS activities were estimated by a modification of the method of Kornberg & Reeves (9) as described previously (13). Cells were harvested, washed twice as described above and stored at −20°C. After thawing, the cells were suspended in 2 mM potassium phosphate buffer (pH 7.0) containing 150 mM KCl and 5 mM $MgCl_2$ ($OD_{660}$ ≈ 5.0). Toluene was added at a final concentration of 1% to the cell suspension, and mixed vigorously for 1 min. After centrifugation (1200 × *g* for 3 min), the cells were suspended in the same buffer ($OD_{660}$ ≈ 50). The PEP-PTS activities for glucose, xylitol or fructose at pH 7.0 were estimated as a decrease of reduced nicotinamide adenine dinucleotide (NADH) in reaction mixtures containing 0.1 mM NADH, 53 μg of cells (dry weight)/ml, 1 mM phosphoenolpyruvate, 11 U/ml lactate dehydrogenase (EC 1.1.1.27, rabbit muscle; Roche Diagnostics, Indianapolis, IN) and 100 mM potassium phosphate buffer (pH 7.0) at 35°C. The reaction was started by adding 5, 10, 30, 60 or 120 mM glucose, xylitol or fructose. The decrease of NADH was monitored using a dual wavelength spectrophotometer (model 557; Hitachi Ltd, Tokyo, Japan) at 340 nm.

### Inhibition of glucose : PEP-PTS activity in the presence of xylitol

Glucose : PEP-PTS activity in the presence of xylitol was also determined. Toluene-treated cells as described above were suspended in a reaction mixture containing 1 mM NADP, 53 μg of cells [dry weight]/ml, 1 mM phosphoenolpyruvate, 3.5 U/ml glucose 6-phosphate dehydrogenase (EC 1.1.1.49, yeast; Roche Diagnostics) and 100 mM potassium phosphate buffer (pH 7.0) at 35°C. The reaction was started by adding 10 mM glucose and 0, 10, 30, 60 or 120 mM xylitol to the cell suspensions. The increase of NADPH was monitored spectrophotometrically at 340 nm.

### Assays of glycolytic intermediates and xylitol 5-phosphate

Cell suspensions were reacted with 10 mM glucose containing 0 or 30 mM xylitol as described above for the experiment of acid production. After the incubation for 2 min, the cells were collected by passing the reaction mixture through a membrane filter (pore size 0.45 μm, polyethersulfone; Acrodisc, Pall Gelman Laboratory, Ann Arbor, MI). Glycolytic intermediates and xylitol 5-phosphate in the cells were immediately extracted in 0.6 N perchloric acid, and neutralized with 5 M $K_2CO_3$ in air. The neutralized extracts were stored at 4°C for subsequent assays of the glycolytic intermediates and xylitol 5-phosphate, and at −20°C for 3-phosphoglycerate assays.

The glycolytic intermediates in the cell extracts were enzymatically determined at 35°C by a modification of the enzymatic method of Minakami et al. (12). Xylitol 5-phosphate was estimated as described previously (13). The assay mixture for xylitol 5-phosphate contained 1.1 mM NAD, 5 mM $MgCl_2$, 0.1 mM EDTA, and the extracts in 50 mM Tris-HCl buffer (pH 8.5) at 35°C. The reaction was started by the addition of 4.2 U/ml polyol dehydrogenase (EC 1.1.1.14, sorbitol dehydrogenase, sheep liver; Roche Diagnostics) and 50 U/ml alkaline phosphatase (EC 3.1.3.1, calf intestine; Roche Diagnostics). The increase of NADH was monitored spectrophotometrically at 340 nm.

### Statistical methods

Differences in rates of acid production, rates of glucose : PEP-PTS activities with xylitol and in profiles of glycolytic intermediates were analyzed by the Mann–Whitney *U*-test. Differences in amounts of

*Table 1.* Relative rate of acid production and the formation of acidic end products from 10 mM glucose (G) and 10 mM glucose plus 30 mM xylitol (G +X).

| *S. mutans* strain | Substrate | Relative rate of acid production | Acidic end products | | |
|---|---|---|---|---|---|
| | | | Lactate | Acetate | Formate |
| ATCC 31989 | G | 100 [a] | 1.44 ± 0.28[b] | 0.34 ± 0.09 | 0.34 ± 0.06 |
| | G +X | 14 ± 1[#] | 0.07 ± 0.01* | 0.25 ± 0.04 | 0.27 ± 0.04 |
| NCTC 10449 | G | 100 | 1.07 ± 0.07 | 0.92 ± 0.04 | 0.90 ± 0.05 |
| | G +X | 74 ± 9[#] | 0.42 ± 0.03 | 1.00 ± 0.07 | 1.11 ± 0.13 |
| NCIB 11723 | G | 100 | 1.72 ± 0.21 | 0.67 ± 0.08 | 0.75 ± 0.10 |
| | G +X | 102 ± 6 | 1.62 ± 0.22 | 0.69 ± 0.09 | 0.78 ± 0.12 |

[a] Relative rate of acid production (mean ± standard deviation, %) obtained from six independent experiments. Significant difference between relative rates of acid production in the presence and absence of xylitol: #$P < 0.01$.
[b]Amounts of acidic end products (mean ± standard deviation, μmol/mg cells) obtained from three independent experiments. Significant difference between amounts of acidic end products in the presence and absence of xylitol: *$P < 0.05$.

acidic end products were analyzed by the Dunn test.

## Results

### Inhibitory effect of xylitol on acid production

Xylitol significantly inhibited the acid production from glucose of *S. mutans* ATCC 31989 and NCTC 10449. In the presence of 30 mM xylitol, the acid production rates of ATCC 31989 and NCTC 10449 were decreased by 86 ± 1% ($P < 0.01$) and 26 ± 9% ($P < 0.01$), respectively, whereas that of NCIB 11723 was not inhibited (Table 1).

The total amounts of acidic end products generated by ATCC 31989 and NCTC 10449 cells decreased in the presence of xylitol. The reduction of lactic acid was remarkable and it was significant in ATCC 31989 ($P < 0.05$), resulting in an end product shift to formate-acetate-dominant (Table 1). Xylitol had no effect on NCIB11723.

### Glucose, xylitol and fructose : PEP-PTS activities

All *S. mutans* strains had PEP-PTS activities for glucose, xylitol, and fructose (Fig. 1). In ATCC 31989, fructose : PEP-PTS activity at 5–120 mM fructose and xylitol : PEP-PTS activity at 30–120 mM xylitol were higher than glucose : PEP-PTS activity. In particular, xylitol : PEP-PTS activity at 30 mM xylitol was 120 ± 14% of glucose : PEP-PTS activity at 10 mM glucose. In NCTC 10449, both fructose and xylitol : PEP-PTS activities were lower than glucose : PEP-PTS activity. Xylitol : PEP-PTS activity at 30 mM xylitol was 16 ± 6% of glucose : PEP-PTS activity at 10 mM glucose. Both fructose and xylitol : PEP-PTS activities were low in NCIB 11723, and xylitol : PEP-PTS at 30 mM xylitol activity was only 3 ± 1% of glucose : PEP-PTS activity at 10 mM glucose.

### Decrease in glucose : PEP-PTS activity in the presence of xylitol

In the presence of added xylitol, glucose : PEP-PTS activities of ATCC 31989 and NCTC 10449 were decreased (Fig. 2). The presence of 30 mM xylitol decreased glucose : PEP-PTS activity to 67 ± 6 and 83 ± 5%, respectively. As the xylitol concentration increased, the decrease became larger and statistically significant over 60 mM xylitol. However, little inhibition was observed in NCIB 11723.

### Effect of xylitol on the profile of glycolytic intermediates during glucose metabolism

When metabolizing glucose only, all of the *S. mutans* strains had large amounts of fructose 1,6-bisphosphate, but the profiles of glycolytic intermediates downstream of

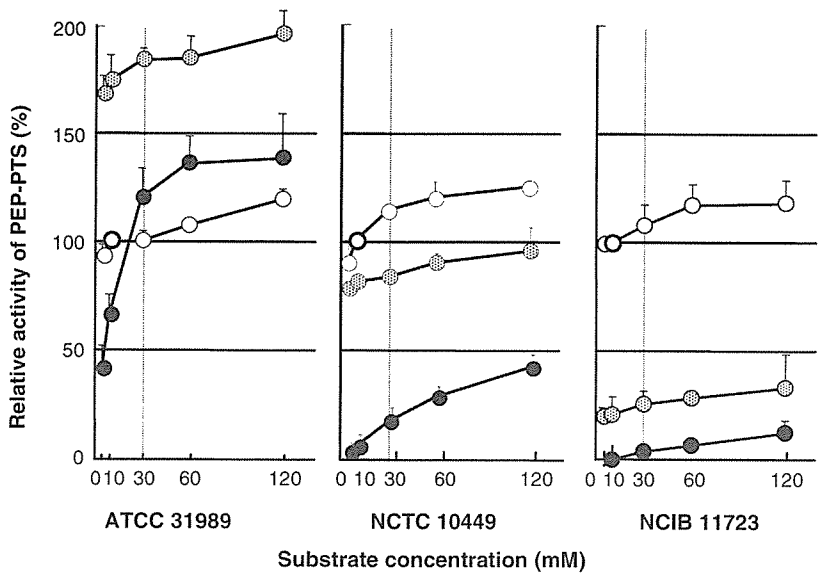


*Fig. 1.* PEP-PTS activities for glucose (○), xylitol (●) and fructose (◍) of *Streptococcus mutans* ATCC 31989, NCTC 10449, and NCIB 11723. Vertical bars indicate standard deviations from three independent experiments. PEP-PTS activity for 10 mM glucose was regarded as 100%.

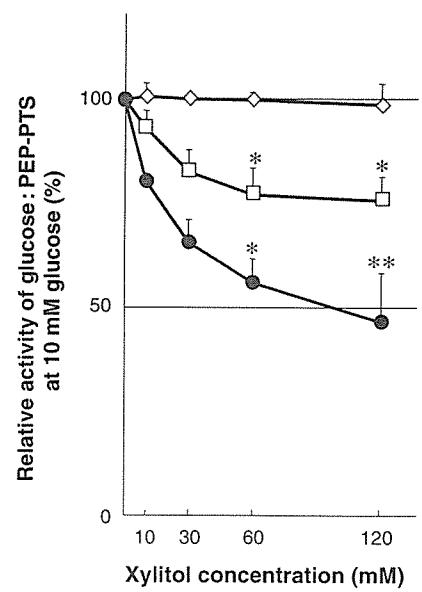


*Fig. 2.* PEP-PTS activities for 10 mM glucose of *Streptococcus mutans* in the presence of xylitol. ATCC 31989 (●), NCTC 10449 (□) and NCIB 11723 (◇). Significant difference between the PEP-PTS activities in the presence and absence of xylitol: *$P < 0.05$, **$P < 0.01$. Vertical bars indicate standard deviations from three independent experiments.

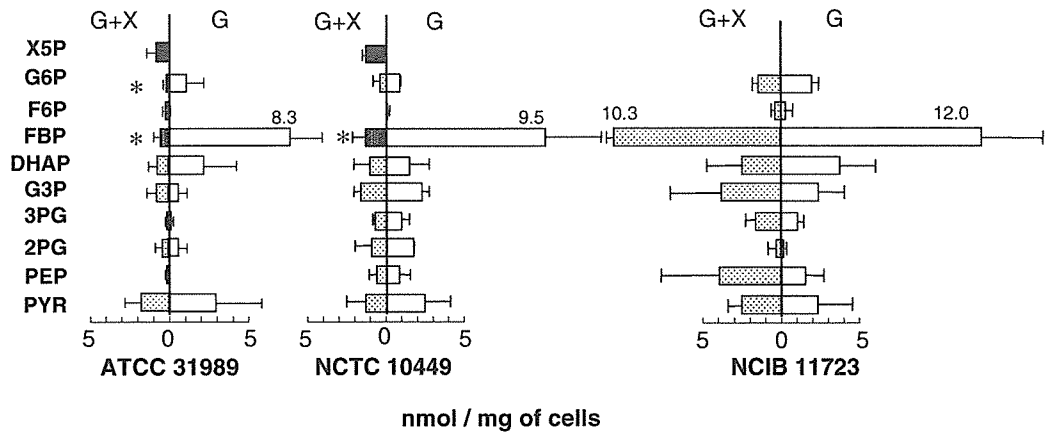


*Fig. 3.* Glycolytic intermediates and xylitol 5-phosphate of *S. mutans* ATCC 31989, NCTC 10449, and NCIB 11723 at 2 min after adding glucose (10 mM) or a mixture of glucose (10 mM) and xylitol (30 mM). Glycolytic intermediates (G, □) in the absence of xylitol. Glycolytic intermediate (G +X, ⊡) and xylitol 5-phosphate (X5P, ■) in the presence of xylitol. G6P, glucose 6-phosphate; F6P, fructose 6-phosphate; FBP, fructose 1,6-bisphosphate; DHAP, dihydroxyacetone phosphate; G3P, glyceraldehyde 3-phosphate; 3PG, 3-phosphoglycerate; 2PG, 2-phosphoglycerate; PEP, phosphoenolpyruvate; PYR, pyruvate. Significant difference between intermediate levels in the presence and absence of xylitol: $*P = 0.05$. Horizontal bars indicate standard deviations from four independent experiments.

dihydroxyacetone phosphate were slightly different among strains (Fig. 3).

When glucose was being metabolized by the ATCC 31989 and NCTC 10449 strains in the presence of xylitol, xylitol 5-phosphate accumulated and the amounts of glycolytic intermediates decreased, particularly those of fructose 1,6-bisphosphate ($P = 0.05$) in ATCC 31989 and NCTC 10449 and glucose 6-phosphate (G6P) ($P = 0.05$) in ATCC 31989. However, such inhibition was not evident in NCIB 11723.

## Discussion

As previously reported (13, 25), xylitol inhibited the acid production of *S. mutans* strains and decreased the lactate production in strains ATCC 31989 and NCTC 10449 (Table 1), but the degree of these inhibitions varied between strains. On the other hand, in strain NCIB 11723, xylitol did not inhibit acid production or shift the end product profile.

Trahan (18) proposed an inhibitory mechanism of xylitol in which *S. mutans* transports xylitol as xylitol 5-phosphate through the activity of xylitol : PEP-PTS and, consequently, the xylitol 5-phosphate inhibits phosphoglucose isomerase and phosphofructokinase, the glycolytic enzymes for G6P conversion to fructose 1,6-bisphosphate, resulting in a decrease in intracellular levels of fructose 1,6-bisphosphate and the entire glycolytic rate. Miyasawa et al. (13) and Maehara et al. (11) then confirmed this notion, and found the decrease in lactate production was due to the decrease in fructose 1,6-bisphosphate, an absolute activator of streptococcal lactate dehydrogenase. The present study found that higher xylitol : PEP-PTS activity indicated more inhibition of acid production by xylitol (Table 1 and Fig. 1). This observation supports the notion that xylitol 5-phosphate produced by xylitol : PEP-PTS activity is responsible for glycolytic inhibition and suggests that *S. mutans* strains with higher xylitol : PEP-PTS activity are more sensitive to xylitol inhibition. It has been proposed that xylitol is transported via a constitutive fructose : PEP-PES and that xylitol : PEP-PTS activity appears as part of the constitutive fructose : PEP-PTS activity (18, 19, 22). We found here that high fructose : PEP-PTS activities in *S. mutans* were accompanied by high xylitol : PEP-PTS activities (Fig. 1), supporting this notion. Furthermore, it is reported that the *fxpC* gene of the constitutive fructose : PEP-PTS was located in the genomes of xylitol-sensitive streptococci and the *fxpC*-defective mutant was resistant to xylitol (2), although no information is available about *fxpC* gene in the strains used in our study.

Analyses of metabolic intermediates revealed that the xylitol-sensitive strains ATCC 31989 and NCTC 10449 accumulated xylitol 5-phosphate and decreased fructose 1,6-bisphosphate in the presence of xylitol (Fig. 3). These results support the notion that xylitol inhibits the glycolytic enzymes required for G6P conversion to fructose 1,6-bisphosphate. Despite the powerful inhibitory effect of xylitol (Table 1) and high xylitol : PEP-PTS activity (Fig. 1), the accumulation of xylitol 5-phosphate in ATCC 31989 seemed to be smaller than that in NCTC 10449. It is suggested that the glycolytic enzymes of ATCC 31989 are more sensitive to xylitol and a small amount of xylitol 5-phosphate is enough to inhibit the entire glycolytic metabolism.

Not only fructose 1,6-bisphosphate but also G6P significantly decreased in a highly xylitol-sensitive strain ATCC 31989 (Fig. 3), indicating that xylitol itself can inhibit the glucose uptake system (e.g. glucose : PEP-PTS) and result in a decrease in intracellular G6P. This was confirmed by the observation that the presence of xylitol decreased the glucose : PEP-PTS activity in xylitol-sensitive strains, ATCC 31989 and NCTC 10449 (Fig. 2). This could be due to competition for the phosphoryl donor, HPr-P, between the glucose and the xylitol : PEP-PTSs. In the ATCC 31989 strain, with high xylitol : PEP-PTS activity and powerful xylitol inhibition of glucose : PEP-PTS activity, HPr-P could phosphorylate xylitol to xylitol 5-phosphate efficiently and result in a direct inhibition by xylitol 5-phosphate on glycolytic enzymes and an indirect inhibition on glucose phosphorylation by HPr-P.

NCIB 11723 isolated from human dental plaque by Carlsson (4) has natural xylitol resistance like other xylitol-resistant strains isolated from xylitol consumers (21, 23). It has been suggested that the xylitol resistance is due to the absence of a constitutive fructose : PEP-PTS by which xylitol is also incorporated, thus preventing xylitol-resistant strains from incorporating xylitol (19, 21). In the present study, NCIB 11723 had little xylitol : PEP-PTS

activity (Fig. 1) and did not accumulate xylitol 5-phosphate (Fig. 3) in the presence of a low concentration of xylitol, supporting this notion. As the xylitol concentration increased, however, xylitol : PEP-PTS activities of NCIB 11723 appeared (Fig. 1). In the presence of 120 mM xylitol, the xylitol : PEP-PTS activity compared with that of glucose : PEP-PTS reached 12 ± 4%. However, 120 mM xylitol did not inhibit glucose : PEP-PTS activity (Fig. 2) and negligibly inhibited acid production from glucose (data not shown). These findings indicate that xylitol has less affinity for HPr-P than glucose in NCIB 11723. Thus, the strain cannot incorporate xylitol as xylitol 5-phosphate in the presence of both xylitol and glucose.

In conclusion, xylitol sensitivity varies among *S. mutans* strains: the higher the xylitol : PEP-PTS activity, and the more effectively xylitol decreases glucose : PEP-PTS activity, the more sensitive the strain is to xylitol. Xylitol has two inhibitory mechanisms:

- direct inhibition of glycolytic enzymes by xylitol 5-phosphate derived from xylitol : PEP-PTS;
- possibly, indirect inhibition of sugar uptake through competition for the phosphoryl donor, HPr-P, between the glucose and the xylitol : PEP-PTS.

## Acknowledgments

This study was supported in part by a research fellowship (no. 16·3025 to HH) and Grants-in-Aid for Scientific Research (B) (no. 16390601 to NT) from the Japan Society for the Promotion of Science.

## References

1. Assev S, Wåler SM, Rölla G. Further studies on the growth inhibition of some oral bacteria by xylitol. Acta Pathol Microbiol Immunol Scand [B] 1983: **91**: 261–265.
2. Benchabane H, Lortie LA, Buckley ND, Trahan L, Frenette M. Inactivation of the *Streptococcus mutans fxpC* gene confers resistance to xylitol, a caries-preventive natural carbohydrate sweetener. J Dent Res 2002: **81**: 380–386.
3. Bradshaw DJ, Marsh PD. Effect of sugar alcohols on the composition and metabolism of a mixed culture of oral bacteria grown in a chemostat. Caries Res 1994: **28**: 251–256.
4. Carlsson J. Presence of various types of non-haemolytic streptococci in dental plaque and in other sites of the oral cavity in man. Odontol Revy 1967: **18**: 55–74.
5. Gauthier L, Vadeboncoeur C, Mayrand D. Loss of sensitivity to xylitol by *Streptococcus mutans* LG-1. Caries Res 1984: **18**: 289–295.
6. Gehring F, Mäkinen KK, Larmas M, Scheinin A. Turku sugar studies. IV. An intermediate report on the differentiation of polysaccharide-forming streptococci (*S. mutans*). Acta Odontol Scand 1974: **32**: 435–444.
7. Kakuta H, Iwami Y, Mayanagi H, Takahashi N. Xylitol inhibition of acid production and growth of mutans streptococci in the presence of various dietary sugars under strictly anaerobic conditions. Caries Res 2003: **37**: 404–409.
8. Kenney EB, Ash MM. Oxidation reduction potential of developing plaque, periodontal pockets and gingival sulci. J Periodontol 1969: **40**: 630–633.
9. Kornberg HL, Reeves RE. Inducible phosphoenolpyruvate-dependent hexose phosphotransferase activities in *Escherichia coli*. Biochem J 1972: **128**: 1339–1344.
10. Lengeler JW, Jahreis K, Wehmeier UF. Enzymes II of the phosphoenolpyruvate-dependent phosphotransferase systems: their structure and function in carbohydrate transport. Biochim Biophys Acta 1994: **1188**: 1–28.
11. Maehara H, Iwami Y, Mayanagi H, Takahashi N. Synergistic inhibition by combination of fluoride and xylitol on glycolysis by mutans streptococci and its biochemical mechanism. Caries Res 2005: **39**: 521–528.
12. Minakami S, Suzuki C, Saito T, Yoshikawa H. Studies on erythrocyte glycolysis. I. Determination of the glycolytic intermediates in human erythrocytes. J Biochem 1965: **58**: 543–550.
13. Miyasawa H, Iwami Y, Mayanagi H, Takahashi N. Xylitol inhibition of anaerobic acid production by *Streptococcus mutans* at various pH levels. Oral Microbiol Immunol 2003: **18**: 215–219.
14. Postma PW, Lengeler JW, Jacobson GR. Phosphoenolpyruvate: carbohydrate phosphotransferase systems of bacteria. Microbiol Rev 1993: **57**: 543–594.
15. Rogers AH, Pilowsky KA, Zilm PS, Gully NJ. Effects of pulsing with xylitol on mixed continuous cultures of oral streptococci. Aust Dent J 1991: **36**: 231–235.
16. Rölla G, Oppermann RV, Waaler SM, Assev S. Effect of aqueous solutions of sorbitol-xylitol on plaque metabolism and on growth of *Streptococcus mutans*. Scand J Dent Res 1981: **89**: 247–250.
17. Takahashi N, Abbe K, Takahashi-Abbe S, Yamada T. Oxygen sensitivity of sugar metabolism and interconversion of pyruvate formate-lyase in intact cells of *Streptococcus mutans* and *Streptococcus sanguis*. Infect Immun 1987: **55**: 652–656.
18. Trahan L. Xylitol: a review of its action on mutans streptococci and dental plaque – its clinical significance. Int Dent J 1995: **45**: 77–92.
19. Trahan L, Bareil M, Gauthier L, Vadeboncoeur C. Transport and phosphorylation of xylitol by a fructose phosphotransferase system in *Streptococcus mutans*. Caries Res 1985: **19**: 53–63.
20. Trahan L, Bourgeau G, Breton R. Emergence of multiple xylitol-resistant (fructose PTS-) mutants from human isolates of mutans streptococci during growth on dietary sugars in the presence of xylitol. J Dent Res 1996: **75**: 1892–1900.
21. Trahan L, Mouton C. Selection for *Streptococcus mutans* with an altered xylitol transport capacity in chronic xylitol consumers. J Dent Res 1987: **66**: 982–988.
22. Trahan L, Neron S, Bareil M. Intracellular xylitol-phosphate hydrolysis and efflux of xylitol in *Streptococcus sobrinus*. Oral Microbiol Immunol 1991: **6**: 41–50.
23. Trahan L, Soderling E, Drean MF, Chevrier MC, Isokangas P. Effect of xylitol consumption on the plaque-saliva distribution of mutans streptococci and the occurrence and long-term survival of xylitol-resistant strains. J Dent Res 1992: **71**: 1785–1791.
24. Vadeboncoeur C, St Martin S, Brochu D, Hamilton IR. Effect of growth rate and pH on intracellular levels and activities of the components of the phosphoenolpyruvate: sugar phosphotransferase system in *Streptococcus mutans* Ingbritt. Infect Immun 1991: **59**: 900–906.
25. Vadeboncoeur C, Trahan L, Mouton C, Mayrand D. Effect of xylitol on the growth and glycolysis of acidogenic oral bacteria. J Dent Res 1983: **62**: 882–884.

Histochem Cell Biol (2006) 126: 371–380
DOI 10.1007/s00418-006-0171-8

ORIGINAL PAPER

**Hidetoshi Mitani · Ichiro Takahashi · Kazuyuki Onodera**
**Jin-Wan Bae · Takuichi Sato · Nobuhiro Takahashi**
**Yasuyuki Sasano · Kaoru Igarashi · Hideo Mitani**

# Comparison of age-dependent expression of aggrecan and ADAMTSs in mandibular condylar cartilage, tibial growth plate, and articular cartilage in rats

Accepted: 2 March 2006 / Published online: 1 April 2006


**Abstract** A disintegrin and metalloproteinase with thrombospondin motif (adamalysin–thrombospondins, ADAMTS) degrades aggrecan, one of the major extracellular matrix (ECM) components in cartilage. Mandibular condylar cartilage differs from primary cartilage, such as articular and growth plate cartilage, in its metabolism of ECM, proliferation, and differentiation. Mandibular condylar cartilage acts as both articular and growth plate cartilage in the growing period, while it remains as articular cartilage after growth. We hypothesized that functional and ECM differences between condylar and primary cartilages give rise to differences in gene expression patterns and levels of aggrecan and ADAMTS-1, -4, and -5 during growth and aging. We employed in situ hybridization and semiquantitative RT-PCR to identify mRNA expression for these molecules in condylar cartilage and primary cartilages during growth and aging. All of the ADAMTSs presented characteristic, age-dependent expression patterns and levels among the cartilages tested in this study. ADAMTS-5 mainly contributed to ECM metabolism in growth plate and condylar cartilage during growth. ADAMTS-1 and ADAMTS-4 may be involved in ECM turn over in articular cartilage. The results of the present study reveal that ECM metabolism and expression of related proteolytic enzymes in primary and secondary cartilages may be differentially regulated during growth and aging.

**Keywords** ADAMTS · Aggrecan · Mandibular condylar cartilage · Articular cartilage · Growth plate · Growth · Aging

H. Mitani · I. Takahashi (✉) · K. Onodera · J. W. Bae
K. Igarashi · H. Mitani
Division of Orthodontics and Dentofacial Orthopedics,
Tohoku University Graduate School of Dentistry,
4-1 Seiryo-machi, Aoba-ku, Sendai, 980-8575, Japan
E-mail: takahasi@mail.tains.tohoku.ac.jp
Tel.: +81-22-7178374
Fax: +81-22-7178378

T. Sato · N. Takahashi
Division of Oral Ecology and Biochemistry, Tohoku University
Graduate School of Dentistry, 4-1 Seiryo-machi, Aoba-ku,
Sendai, 980-8575, Japan

Y. Sasano
Division of Craniofacial Development and Regeneration,
Tohoku University Graduate School of Dentistry,
4-1 Seiryo-machi, Aoba-ku, Sendai, 980-8575, Japan

K. Igarashi
Division of Oral Dysfunction Science, Tohoku University
Graduate School of Dentistry, 4-1 Seiryo-machi, Aoba-ku,
Sendai, 980-8575, Japan

## Introduction

Aggrecanase is a member of the metalloproteinase family which degrades a major cartilaginous extracellular matrix (ECM) component, aggrecan (Abbaszade et al. 1999; Arner et al. 1999; Tortorella et al. 1999; Caterson et al. 2000; Tang 2001; Arner 2002). Three members of the adamalysin–thrombospondins (ADAMTSs), ADAMTS-1, -4 (aggrecanase-1), and -5 (aggrecanase-2), are capable of cleaving an aggrecan molecule (Abbaszade et al. 1999; Tortorella et al. 1999; Kuno et al. 2000) at its specific sites, in a different manner from matrix metalloproteinases (MMPs), another large family of ECM degrading enzymes. Together with MMPs, ADAMTSs play a role in cartilage ECM metabolism during the development of cartilage and progression of joint diseases (Lohmander et al. 1993; Fosang et al. 1996; Lark et al. 1997; Caterson et al. 2000; Sandy and Verscharen 2001). Most studies have focused on the activity of aggrecanases, especially their production and activation under disease conditions, such as inflammatory responses and joint diseases, whereas their physiological expression patterns have not been determined during growth and aging.

Synovial joints are classified into two types, primary joints, such as the knee, and secondary joints, such as the temporomandibular joint (TMJ) (Ten Cate 1994). In

primary joints, primary articular and growth plate cartilages function separately for articulation and growth, respectively, whereas mandibular condylar cartilage performs both of these functions during growing period. ECM components and cellular organization of mandibular condylar cartilage, as a secondary cartilage, are different from those of primary cartilages as demonstrated previously (Silbermann et al. 1987; Luder et al. 1988; Mizoguchi et al. 1992). While mandibular condylar cartilage has been shown to have five distinct layers, primary cartilages, including growth plate and articular cartilage, is composed of four layers during the growth period (Luder et al. 1988; Mizoguchi et al. 1992). Primary cartilage cells express both type II collagen and aggrecan, cartilage-specific ECM components; however, cells in the upper two layers of mandibular condylar cartilage do not express either of these molecules (Mizoguchi et al. 1992; Takahashi et al. 1996; Shibata et al. 2001). Proliferating cells in growth plate and articular cartilage are well-differentiated chondrocytes, but those in mandibular condylar cartilage are not (Mizoguchi et al. 1992). Thus, cell proliferation and matrix synthesis in mandibular condylar cartilage are regulated differently from those of primary cartilages. In addition, during the growth, development, and maturation of the synovial joints, growth plate cartilage disappears by the end of the growth period. Similar to articular cartilage, which remains in the epiphysis of long bones, mandibular condylar cartilage becomes articular cartilage by losing hypertrophic chondrocytes after growth. Therefore, it can be considered that ECM metabolism in primary and mandibular condylar cartilage is differently regulated.

In this study, we examined the hypothesis that functional and ECM differences between condylar and primary cartilage give rise to differences in gene expression patterns and levels of ADAMTS-1, -4, and -5 during growth and aging. To test this hypothesis we used semiquantitative reverse transcriptase polymerase chain reaction (RT-PCR) and in situ hybridization (ISH) using a newly identified rat ADAMTS-5 mRNA and subcloned aggrecan, ADAMTS-1 and ADAMTS-4.

## Materials and methods

### Experimental animals and tissue preparation

Male Wistar rats 4, 8, 16, and 32 weeks old were used in this study. Five animals for each age group were perfused via the ascending aorta with 4% paraformaldehyde and 0.5% glutaraldehyde in phosphate-buffed saline (PBS), pH 7.4, under pentobarbital anesthesia as described previously (Sasano et al. 1996). Procedures for tissue preparation were basically identical to our previous report (Bae et al. 2003). After the animals were perfused, TMJs and knee joints were dissected, further fixed in the same fixatives, and decalcified in 10% ethylene diamine tetra-acetic acid (EDTA). They were dehydrated, embedded in paraffin, and 8-μm-thick sagittal sections were cut for ISH analysis under RNase-free conditions and hematoxylin and eosin (H&E) staining. Animal experiments were conducted under the approval of the Animal Care and Use Committee of Tohoku University, Japan.

### Cloning aggrecan and ADAMTSs and generating cRNA probes

Reverse transcriptase polymerase chain reaction-based cloning was employed to obtain partial or full clones of each molecule. Based on the homology between mouse and human ADAMTS-5 cDNA sequences, degenerate amplimers were designed as shown in Table 1. For other molecules, amplimers were designed based on the cDNA sequences of rats shown in Table 1 and in our previous study (Nakamura et al. 2005). PCR conditions used in the present study are also summarized in Table 1. The cDNA fragments obtained were subcloned into pCRII-TOPO vector (Invitrogen, Carlsbad, CA, USA), according to the manufacturer's instructions. Nucleic acid sequences of ADAMTS-5 were analyzed by the dye-terminating method using ALF express II sequencer (Amersham Pharmacia Biotech, Buckinghamshire, UK) and the other fragments were analyzed by Takara (Osaka, Japan) to confirm the nucleic acid sequences. To create Dig-labeled riboprobes for sense and antisense fragments, the plasmids were linearized and transcribed by using Sp6 or T7 RNA polymerases (Stratagene, La Jolla, CA, USA) into cRNA as indicated in Table 1.

### In situ hybridization

The protocol for ISH has been described previously (Ohtani et al. 1992; Sasano et al. 1996; Zhu et al. 2001). Sections were deparaffinized, rehydrated, and immersed in 0.2 N HCl for 20 min at room temperature, then incubated with 20 μg/ml proteinase K (Roche Diagnostics, Indianapolis, IN, USA) at 37°C for 30 min. After sections were dehydrated in ethanol, they were hybridized with approximately 400 ng/ml riboprobes at 45°C for 16 h. Sections were incubated with 20 μg/ml RNase A (Sigma, St Louis, MO, USA) in 1× SSC (saline–sodium citrate buffer) during stringent wash in 2× SSC and 1× SSC at 45°C. After sections were incubated with anti-Dig alkaline phosphatase-conjugated antibody (Roche Diagnostics) at 4°C overnight in a moisture chamber, signals were visualized and nuclear counterstaining was performed using methyl green. Sections were mounted and observed under light microscopy.

### Semiquantitative RT-PCR

Gene expression of aggrecan and ADAMTS-1, -4, and -5 were semiquantified by RT-PCR in three types of cartilage. Bilateral mandibular condylar, growth plate, and articular cartilages were dissected from 4-week-old and adult male Wistar rats killed by ether anesthesia.

**Table 1** Conditions for cloning, creating riboprobes and semi-quantitative RT-PCR

| Gene name and accession no. | Nucleic acid sequences of amplimers | PCR annealing temperature(°C) | Product length (bp) | Cycle number for semi-quantitative RT-PCR | Restriction enzymes for | | RNA polymerase |
|---|---|---|---|---|---|---|---|
| Aggrecan | Upstream GTTAGTGGAGGGCGTGAC | 55 | 634 | 32 cycles | Anti-sense | *Eco*RV | Sp6 |
| NM_022190 | Downstream CTTGGCTGTTTCTGCTGTT | | | | Sense | *Bam*HI | T7 |
| ADAMTS-1 | Upstream-1 GTTGGGAAAGGAAAGCAGA | 68 | 1,123 | – | Anti-sense | *Eco*RV | Sp6 |
| NM_024400 | Downstream-1 AGGGTTGTGGCAGGAAATA | | | | Sense | *Bam*HI | T7 |
| | Upstream-2 GGCGGAGGACGAAGAGT | 62 | 445 | 48 cycles | – | – | – |
| | Downstream-2 GGAAGCGAGGAGTAGCAAC | | | | | | |
| ADAMTS-4 | Upstream CTACAACCACCGAACCGAC | 60 | 602 | 48 cycles | Anti-sense | *Spe*I | T7 |
| XM_237904 | Downstream TGCCAGCCACCAGAACTT | | | | Sense | *Eco*RV | Sp6 |
| ADAMTS-5 | Upstream-1 ATGCKNCTYGRNTGGGC | 60 | 1,395 | – | NA | NA | NA |
| AF142099 | Downstream-1 ACCGTCATCCAGAAATTC | | | | NA | NA | NA |
| NM_011782 | Upstream-2 GATCTCTAGAATCATTCATG TGACACCCTG | 60 | 1,685 | – | Anti-sense | *Spe*I | Sp6 |
| | Downstream-2 GATCTCTAGAAACCACAGGCT AACATTTC | | | | Sense | *Xho*I | T7 |
| | Upstream-3 GGCTGTGGTGTGCTGTG | 58 | 758 | 48 cycles | – | – | – |
| | Downstream-3 CTGGTCTTTGGCTTTGAAC | | | | | | |
| GAPDH | Upstream TGTTTGTGATG GTGTGAA | 56 | 485 | 30 cycles | – | – | – |
| MN_017008 | Downstream ATGGGAGTTGCTGTTGAG | | | | | | |

Mandibular condyles and tibial epiphysis were removed from mandibular bone and tibia, respectively. Cartilaginous tissues in the articular surfaces of mandibular condyle and tibia were removed carefully under dissection microscope in ice-cold PBS by using fine scalpels. After articular cartilage was obtained, bone tissue in secondary ossification center and cartilaginous tissue fragments of remained articular cartilage were carefully removed, then growth plates were separated from tibial epiphysis of 4-week-old rats. The specimens were frozen in liquid nitrogen and homogenized in lysis buffer to isolate total RNA using the RNeasy Lipid Tissue Mini Kit (Qiagen, Hilden, Germany) following the manufacturer's instructions. Standardized 200 ng amounts of total RNA were reverse transcribed before PCR amplification. PCR conditions and number of reaction cycles were empirically determined by drawing amplification curves at each annealing temperature for each molecule (Table 1). Optical density from each amplified product separated on 2% agarose gel was digitized and measured using NIH imaging software (National Institutes of Health, Bethesda, MD, USA), and relative gene expression levels were semi-quantified against glyceraldehyde-3-phosphate dehydrogenase. Expression levels were statistically analyzed by Scheffe's test.

## Results

### Cloning rat ADAMTS-5

The deduced amino acid sequence of rat ADAMTS-5 is shown in Fig. 1, aligned with human and mouse ADAMTS-5. The coding sequence of rat ADAMTS-5 mRNA consists of 2,787 bp (GenBank Accession No. AY382879), which generates 928 amino acid residues. Rat ADAMTS-5 mRNA had 93.6 and 84.9% homology with that of mice and humans, respectively. The amino acid sequence of rat ADAMTS-5 showed 96.2 and 90.3% homology to that of mice and humans, respectively. Rat ADAMTS-5 protein lacked two amino acid residues in the metalloproteinase domain at $Asp^{326}$ and $Thr^{327}$ when compared to mouse ADAMTS-5. Pre- and pro-domains were less conserved in rats when compared to mice or humans. The domain structure of ADAMTS-5 in rats was identical to that in other species with a metalloproteinase domain including a catalytic domain, two thrombospondine-1 motifs, and a disintegrin-like motif.

### Histological observation (Figs. 2, 3)

During the growth period, mandibular condylar cartilage consisted of five cell layers: a fibrous layer with fibroblasts embedded in the fibrous connective tissue, a proliferative cell layer with undifferentiated and proliferating polygonal cells, a transitional cell layer with flattened cells without cytosolic lipid droplets, a mature cell layer, and a hypertrophic cell layer (Fig. 2a, b). Tibial

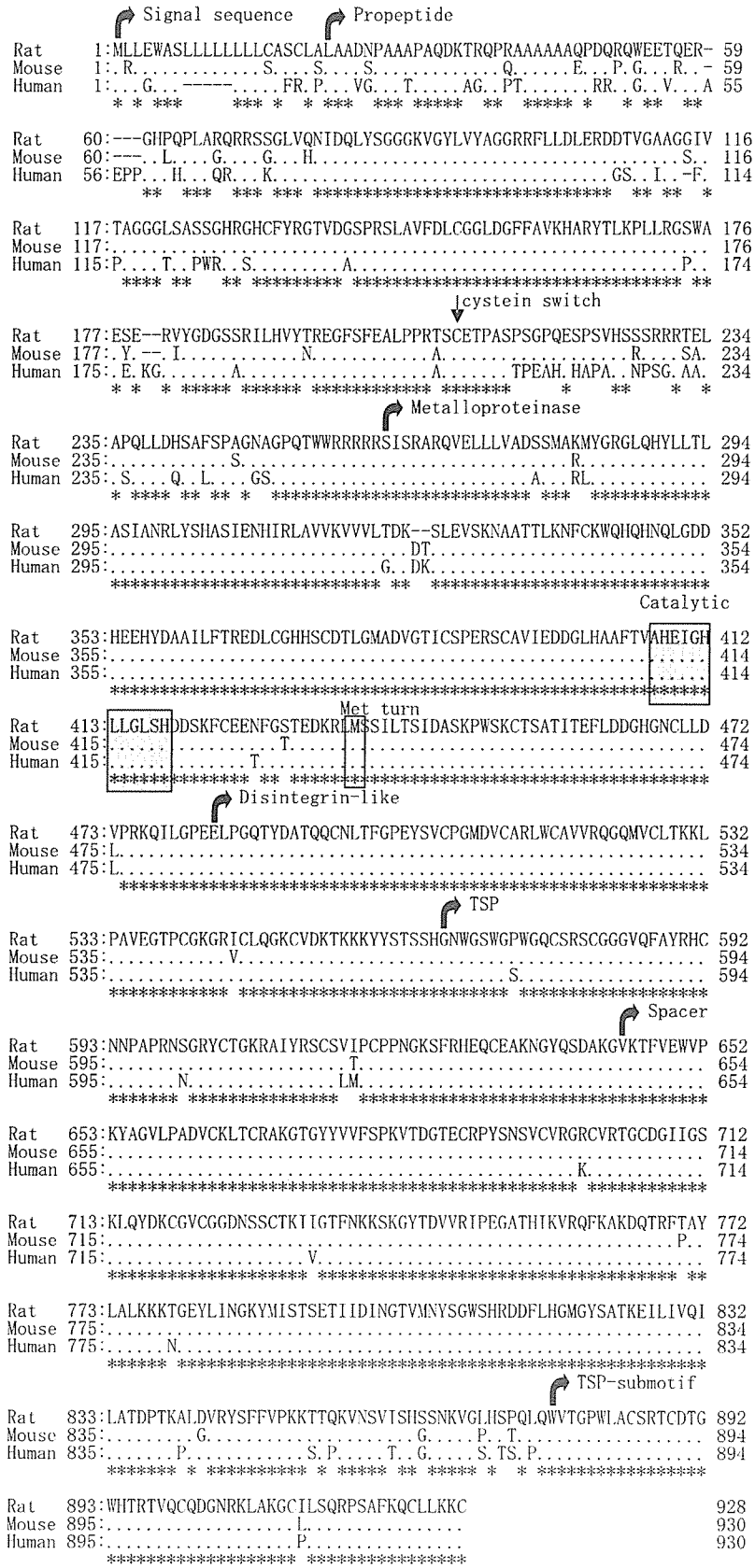


**Fig. 1** The amino acid sequence deduced from the ADAMTS-5 cDNA is shown aligned with those of human and mouse ADAMTS-5. Residues matching the consensus sequence of the three proteins are *dotted* in the human and mouse sequences. The conserved zinc-binding motif and "Met turn" are *boxed*. *TSP* thrombospondin motif

epiphyseal growth plate cartilage and articular cartilage consisted of four layers: a resting cell layer with chondrocytes, which was the smallest in size of all the layers; a proliferative cell layer with flattened, proliferating cells; a mature cell layer containing ovoid-shaped well-differentiated chondrocytes with lipid drops; and a hypertrophic

cell layer consisting of enlarged cells with disorganized cytosolic structures during the growth period (Fig. 3a, b). Mandibular condylar cartilage showed characteristics of growth plate cartilage with a hypertrophic cell layer at the lower border involved in endochondral bone formation during growth. In contrast, mandibular condylar cartilage at 16 and 32 weeks of age mainly consisted of three layers: a resting cell layer, a proliferating cell layer, and a mature cell layer (Fig. 2c, d), and closely resembled articular cartilage lacking the hypertrophic cell layer seen in younger animals (Fig. 3c). The uppermost layer of aged mandibular condylar cartilage was a fibrous layer with elongated fibroblasts embedded in fibrous connective tissue, the second layer was a proliferating cell layer consisting of small proliferating cells, and the lower layer was a mature cell layer with well-differentiated chondrocytes, including some hypertrophic cells (Fig. 2c, d). Tibial articular cartilage consisted of three layers at 32 weeks of age (Fig. 3c).

Gene expression patterns (Figs. 4, 5, 6)

*Age 4 and 8 weeks (Figs. 4, 5)*

At 4 and 8 weeks of age, positive hybridization signals for aggrecan were observed in mature and hypertrophic chondrocytes in condylar, articular, and the growth plate cartilage (Figs. 4a, e, 5a, e). While condylar cartilage did not show positive signals for aggrecan in the upper three layers (Fig. 4a, e), a positive signal was observed in the resting and proliferating cell layers in both articular and growth plate cartilage (Fig. 5a, e). ADAMTS-1

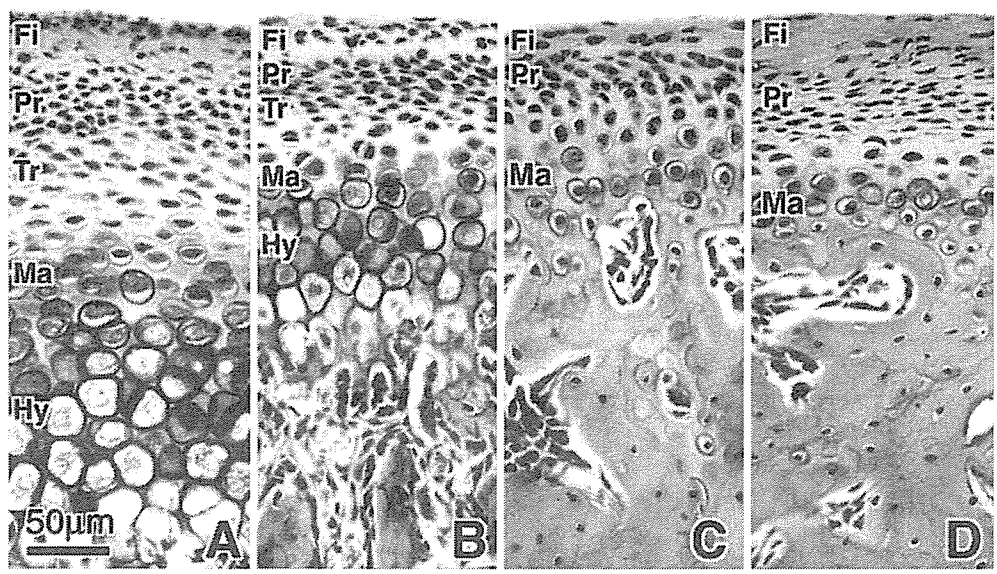


**Fig. 2** Sagittal sections of mandibular condylar cartilage stained with H&E from 4-week-old (**a**), 8-week-old (**b**), 16-week-old (**c**), and 32-week-old (**d**) rats. *Fi* fibrous layer; *Pr* proliferative cell layer; *Tr* transitional cell layer; *Ma* mature cell layer; *Hy* hypertrophic cell layer. *Scale bar* 50 μm; original magnification: ×40

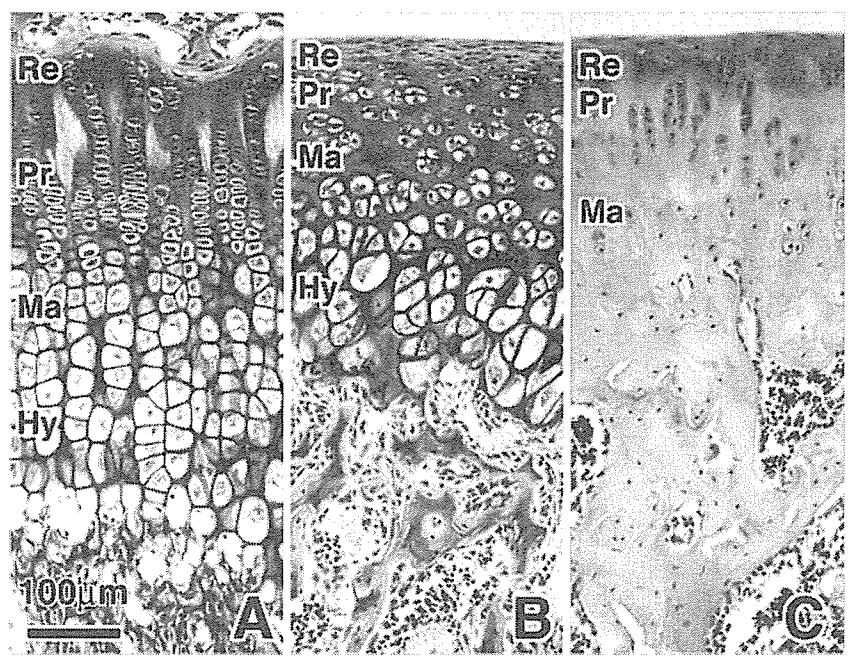


**Fig. 3** Sagittal sections of growth plate and articular cartilage stained with H&E. Growth plate cartilage from 4-week-old rats (**a**) and articular cartilage from 4-week-old (**b**), and 32-week-old (**c**) rats. *Re* resting cell layer; *Pr* proliferative cell layer; *Ma* mature cell layer; *Hy* hypertrophic cell layer. *Scale bar* 100 μm; original magnification: ×20

expression was observed in all of the cell layers in the three types of cartilage during growth (Figs. 4b, f, 5b, f). In condylar cartilage, mature chondrocytes showed the strongest hybridization signals to ADAMTS-1 compared to the other layers at ages 4 and 8 weeks (Fig. 4b, f). The cells in the transitional cell layer and below were positive for ADAMTS-4 in condylar cartilage, with the strongest expression in hypertrophic chondrocytes (Fig. 4c, g). Cells in all four layers showed positive signals for ADAMTS-4 in growing articular cartilage at 4 weeks (Fig. 5g), while cells in the proliferating cell layer were negative in growth plate cartilage (Fig. 5c). ADAMTS-5 showed positive hybridization signals localized in mature and hypertrophic chondrocytes in both condylar (Fig. 4d, h) and growth plate cartilage (Fig. 5d), while it was observed in all cell layers in articular cartilage at 4 weeks of age (Fig. 5h). During the growth period, the expression domain of aggrecan covered that of ADAMTS-5, while other ADAMTSs had a greater expression domain than that of aggrecan, especially ADAMTS-1, which was expressed ubiquitously in all types of cartilage during the growth period. In addition, all types of ADAMTSs were expressed in all four layers of articular cartilage during growth.

*Age 16 and 32 weeks (Fig. 6)*

After growth was completed and the hypertrophic cell layer disappeared, positive hybridization signals for aggrecan were localized in mature chondrocytes of condylar and articular cartilage (Fig. 6a, e, i). With aging, aggrecan expression was maintained in the well-differentiated chondrocytes in the mature cell layers. However, the strength of the hybridization signal decreased with age. The hybridization signal for ADAMTS-1 in the fibrous layer, which was positive at 8 weeks (Fig. 4b, f), was negative at 16 and 32 weeks (Fig. 6b, f). Consequently, the area negative for ADAMTS-1 in condylar cartilage expanded from the fibrous layer to the proliferating cell layer by 32 weeks (Fig. 6b, f). The hybridization signal for ADAMTS-1 remained in all of the cell layers in articular cartilage at 32 weeks of age (Fig. 6j). ADAMTS-4 was

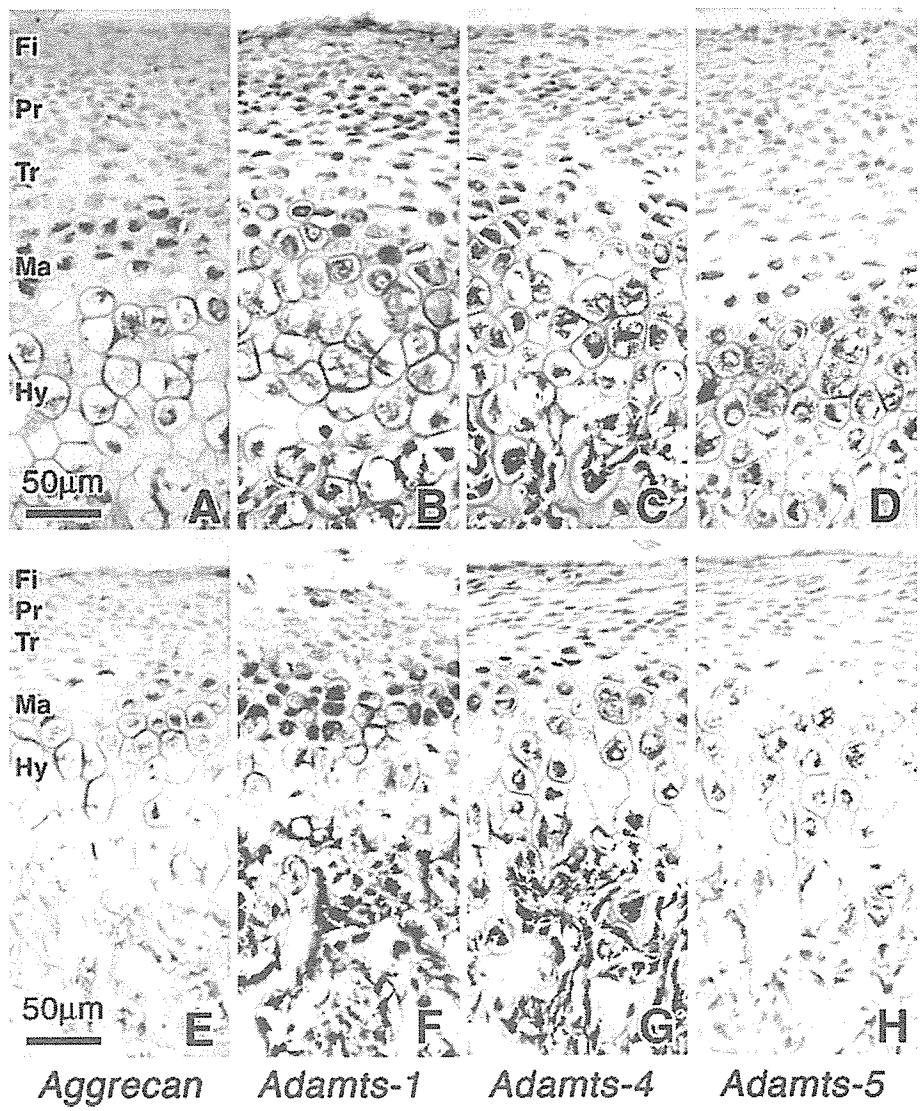


**Fig. 4** In situ hybridization analysis for aggrecan (**a**, **e**), ADAMTS-1 (**b**, **f**), ADAMTS-4 (**c**, **g**), and ADAMTS-5 (**d**, **h**) of sagittal sections of mandibular condylar cartilage from 4-week-old (**a**–**d**) and 8-week-old (**e**–**h**) rats. *Fi* fibrous layer; *Pr* proliferative cell layer; *Tr* transitional cell layer; *Ma* mature cell layer; *Hy* hypertrophic cell layer. Brown-purple staining in the cytosol is a positive hybridization signal. *Scale bar* 50 μm; original magnification: ×40

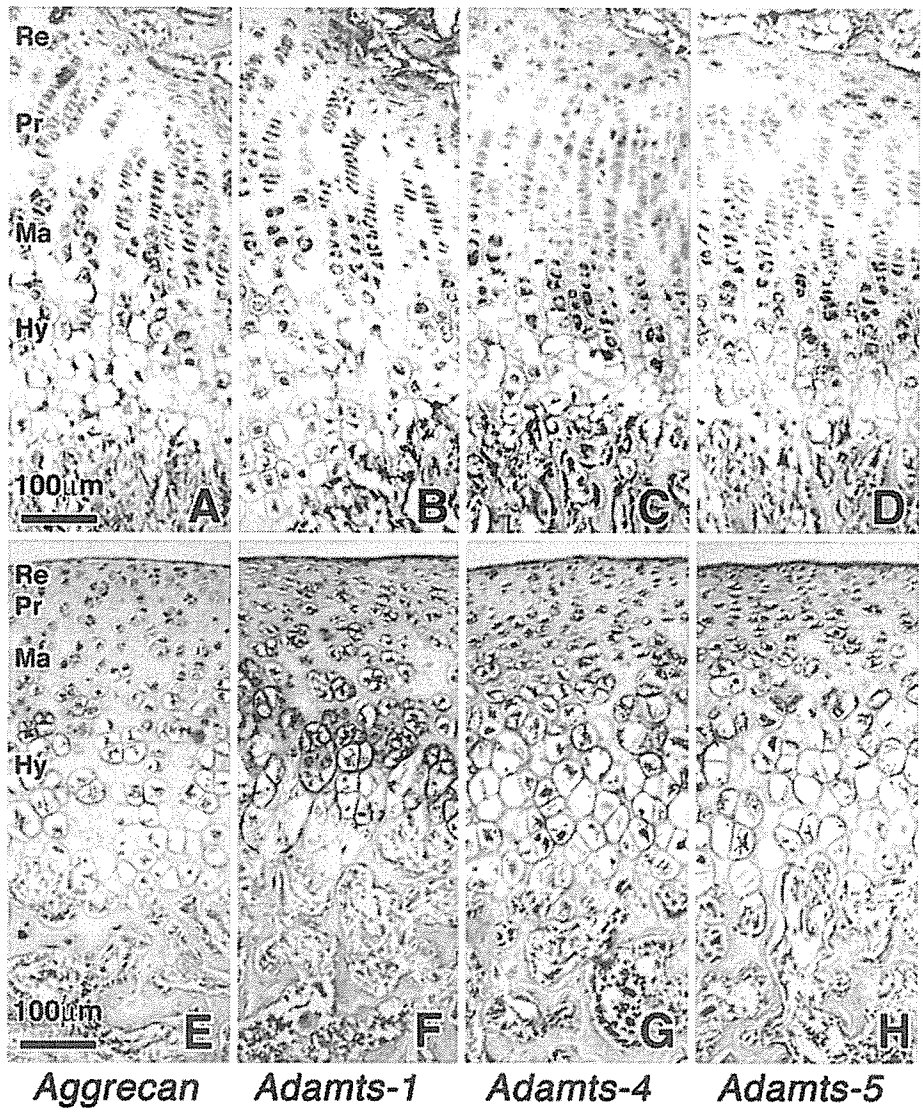


**Fig. 5** In situ hybridization analysis for aggrecan (**a**, **e**), ADAMTS-1 (**b**, **f**), ADAMTS-4 (**c**, **g**), and ADAMTS-5 (**d**, **h**) of sagittal sections of growth plate (**a**–**d**) and articular cartilage (**e**–**h**). *Re* resting cell layer; *Pr* proliferative cell layer; *Ma* mature cell layer; *Hy* hypertrophic cell layer. Brown-purple staining in the cytosol is a positive hybridization signal. *Scale bar* 100 μm; original magnification: ×20

localized in mature chondrocytes at 16 weeks of age (Fig. 6c) and remained so at 32 weeks of age in condylar cartilage (Fig. 6g). It was only localized in mature chondrocytes in articular cartilage (Fig. 6k). ADAMTS-5 was expressed in the lower part of the mature cell layers in condylar cartilage at 16 and 32 weeks (Fig. 6d, h), while it was not expressed in aged articular cartilage (Figs. 6l, 7).

Gene expression levels

The expression level of all ADAMTSs examined was maintained during aging in mandibular condylar cartilage, whereas that of ADAMTS-4 and -5 decreased in articular cartilage during aging (Fig. 7a, b). ADAMTS-4 expression in growth plate cartilage was significantly lower than that in articular cartilage at the same age (Fig. 7a, b). Gene expression levels of aggrecan and ADAMTS-1 were similar in all types of cartilage and at all ages examined, while slightly, but not significantly, less expression of ADAMTS-1 was observed in aged mandibular condylar cartilage (Fig. 7a, b).

## Discussion

ADAMTS-5 is also known as aggrecanase-2, which cleaves aggrecan, one of the cartilage-specific macromolecules (Doege et al. 1991). While all three ADAMTS genes examined have been identified in mice, cattle, and humans, this is the first time that ADAMTS-5 has been identified in rats. Rat ADAMTS-5 conserved all of the domains seen in mice and humans (Abbaszade et al. 1999). Since rat ADAMTS-5 lacks two amino acid residues in the metalloproteinase domain and the catalytic domain is conserved completely when compared to humans and mice, aggrecanase activity of ADAMTS-5 may differ in rats from other species.

The age-dependent changes in aggrecan expression in condylar cartilage were similar to those of type II collagen demonstrated previously (Ohashi et al. 1997; Bae et al. 2003); expression and localization of type II collagen becomes restricted to mature cell layers as aging progresses. In addition, the expression pattern of versican is

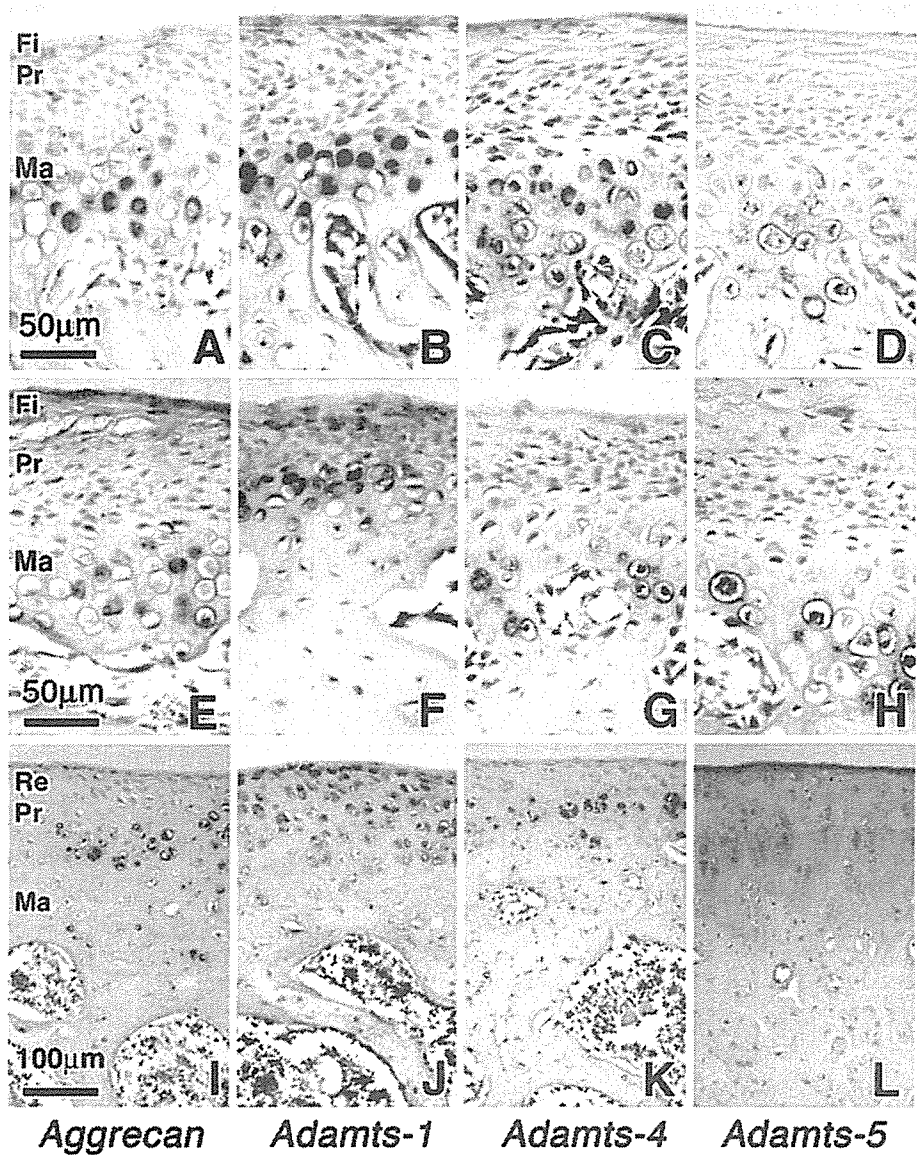


**Fig. 6** In situ hybridization analysis for aggrecan (**a**, **e**, **i**), ADAMTS-1 (**b**, **f**, **j**), ADAMTS-4 (**c**, **g**, **k**), and ADAMTS-5 (**d**, **h**, **l**) of sagittal sections of mandibular condylar cartilage from 16-week-old (**a**–**d**) and 32-week-old (**e**–**h**) rats and articular cartilage from 32-week-old (**i**–**l**) rats. *Re* resting cell layer; *Fi* fibrous layer; *Pr* proliferative cell layer; *Ma* mature cell layer. Brown-purple staining in the cytosol is a positive hybridization signal. *Scale bar* in **a**–**h** 50 μm and **i**–**l** 100 μm; original magnification: ×40 (**a**–**h**) and ×20 (**i**–**l**)

regulated differently in condylar and primary cartilage during growth (Shibata et al. 2001). While versican is co-expressed with aggrecan in primary cartilage, its expression is restricted to the fibrous layer of condylar cartilage, while aggrecan is expressed in the mature and hypertrophic cell layer during embryonic growth. Several researchers have investigated the substrate specificity of the three ADAMTSs: ADAMTS-1 cleaves aggrecan and versican (Kuno et al. 2000; Sandy and Verscharen 2001); ADAMTS-4 cleaves aggrecan, brevican, and versican (Matthews et al. 2000; Nakamura et al. 2000; Tortorella et al. 2000; Sandy and Verscharen 2001; Sztrolovics et al. 2002); and ADAMTS-5 cleaves aggrecan (Abbaszade et al. 1999; Arner 2002). Since ADAMTS-1 is the only ADAMTS among those examined in the present study that is expressed in the fibrous layer of condylar cartilage, it may contribute to versican metabolism in this layer. Thus, specific expression patterns of each ADAMTS may reflect the expression of their specific substrates during endochondral ossification.

Tibial growth plate and mandibular condyle are sites of endochondral bone formation. Chondrocytes in the growth plate and condylar cartilage deposit cartilaginous ECM components such as aggrecan and type II collagen to provide a template that is subsequently replaced by bone tissue. Cell volume increases as chondrocytes differentiate during this process (Luder et al. 1988). Besides the expression of ADAMTSs, chondrocytes produce several types of MMP during growth (Bae et al. 2003; Gepstein et al. 2003). Therefore, once deposited, ECM components such as type II collagen and aggrecan are degraded by aggrecanases in combination with MMPs. ADAMTS-5, mainly expressed in mature and hypertrophic chondrocytes in both condylar and growth plate cartilage, may provide space for expanding chondrocytes during terminal differentiation. In addition, recent studies have demonstrated that targeted